



# Reno-protective effects of ursodeoxycholic acid against gentamicin-induced nephrotoxicity through modulation of NF- $\kappa$ B, eNOS and caspase-3 expressions

Tarek Hamdy Abd-Elhamid<sup>1</sup> · Dalia A. Elgamal<sup>1</sup> · Safaa S. Ali<sup>1</sup> · Fares E. M. Ali<sup>2</sup> · Emad H. M. Hassanein<sup>2</sup> · Ehab A. M. El-Shoura<sup>2</sup> · Ramadan A. M. Hemeida<sup>2</sup>

Received: 27 December 2017 / Accepted: 4 July 2018 / Published online: 4 August 2018  
© Springer-Verlag GmbH Germany, part of Springer Nature 2018

## Abstract

Gentamicin (GNT) is a potent aminoglycoside antibiotic widely used to treat life-threatening bacterial infections. We aim to investigate the potential protective effect of ursodeoxycholic acid (UDCA) against GNT-induced nephrotoxicity. In this study, 24 male Wistar rats were used and randomly divided into four groups of six animals each. Control group received 0.5% carboxymethyl cellulose orally for 15 days, GNT group received GNT 100 mg/kg/day i.p. for 8 days, UDCA group received UDCA orally for 15 consecutive days at a dose of 60 mg/kg/day suspended in 0.5% carboxymethyl cellulose and UDCA-pretreated group received UDCA orally for 7 days then co-administered with GNT i.p. for 8 days at the same fore-mentioned doses. Serum levels of kidney function parameters (urea, creatinine, uric acid and albumin) were measured. Renal tissues were used to evaluate oxidative stress markers; malonaldehyde (MDA), reduced glutathione (GSH) and the anti-oxidant enzyme superoxide dismutase (SOD) activities and nuclear factor kappa light-chain enhancer of activated B cells (NF- $\kappa$ B) and kidney injury molecule-1 (KIM-1) mRNA levels. Immunohistochemical expression of endothelial nitric oxide synthase (eNOS) and caspase-3 and histological and ultrastructural examination were performed. Treatment with GNT increased the serum levels of renal function parameters and renal MDA, NF- $\kappa$ B and KIM-1 mRNA levels, while it decreased GSH and SOD activities. Marked immunohistochemical expression of caspase-3 was observed after GNT administration while it decreased eNOS expression. Histological and ultrastructural alterations were also evident in renal corpuscles and tubules. In contrast, pretreatment with UDCA reversed changes caused by GNT administration. These results suggest that UDCA ameliorates GNT-induced kidney injury via inhibition of oxidative stress, inflammation and apoptosis.

**Keywords** Ursodeoxycholic acid · Gentamicin · NF- $\kappa$ B · eNOS · Caspase-3

## Introduction

Gentamicin (GNT) is an aminoglycoside antibiotic widely used for the treatment of serious infections caused by various

Gram-negative bacteria. Its bactericidal effect is through binding of prokaryotic ribosomes that leads to mistranslation and inhibition of protein synthesis (Davies and Davis 1968). Despite its powerful bactericidal effect, its clinical use is

✉ Tarek Hamdy Abd-Elhamid  
tabdelhamid@aun.edu.eg; tarekgobara@yahoo.com

Dalia A. Elgamal  
delgamal1974@yahoo.com

Safaa S. Ali  
hassan.safaa@yahoo.com

Fares E. M. Ali  
fares\_aly888@yahoo.com

Emad H. M. Hassanein  
emad\_pharma2013@yahoo.com

Ehab A. M. El-Shoura  
dr\_ehabalshoura@yahoo.com

Ramadan A. M. Hemeida  
ramadanhemeida@yahoo.com

<sup>1</sup> Department of Histology and Cell Biology, Faculty of Medicine, Assiut University, Assiut, Egypt

<sup>2</sup> Department of Pharmacology, Faculty of Pharmacy, Al-Azhar University, Assiut, Egypt

limited due to its toxic effects on various tissues including the kidney. Although most of the administered dose of GNT is excreted in urine, a small fraction of GNT accumulates in the renal cortex and remains there even after discontinuation of GNT administration (Akao et al. 2002; Nagai and Takano 2004). Unfortunately, 24% of patients who were treated with GNT for more than 7 days developed renal damage (Selby et al. 2009).

Gentamicin-induced nephrotoxicity is characterized by tubular damage and renal dysfunction. These toxic effects are related to the selective accumulation of GNT within the proximal convoluted tubules in human (Luft et al. 1977) as well as experimental animals (Pattyn et al. 1988) reaching a concentration of 50 to 100 times greater than serum. This is because GNT is endocytosed through receptor-mediated endocytosis by megalin, a membrane glycoprotein present in the apical membrane of the proximal convoluted tubules (Nagai and Takano 2004; Watanabe et al. 2004). In proximal tubular cells, GNT accumulates in the lysosomes (El Mouedden et al. 2000) and passes in a retrograde manner through the Golgi complex and endoplasmic reticulum to the cytoplasm (Sandoval and Molitoris 2004). The accumulation of GNT in the proximal tubules leads to structural changes ranging from loss of brush border to tubular necrosis (Sardana et al. 2015; Whiting and Brown 1996).

The exact mechanism of GNT-induced nephrotoxicity is not well-known. Previous experiments have linked GNT-induced nephrotoxicity and oxidative stress. In this regard, GNT reduces the anti-oxidant defense mechanisms and increases the production of free radicals in the kidney, such as superoxide anion, hydroxyl radicals, hydrogen peroxide and reactive nitrogen species (Abdel-Raheem et al. 2009; Balakumar et al. 2010). These free radicals destroy the tubular epithelial cells, which in turn leads to defective tubular reabsorption and kidney dysfunction (Baliga et al. 1999; Maldonado et al. 2003). Other data suggested involvement of renal inflammation in GNT-induced kidney damage. This includes inflammatory cell infiltration, increased expression of inducible nitric oxide synthase (iNOS) and nuclear localization of the nuclear factor kappa light-chain enhancer of activated B cells (NF- $\kappa$ B) in renal tissue of GNT-treated animals (Bae et al. 2014). Furthermore, activation of the apoptotic pathways has been shown underlining GNT-induced renal damage (Bae et al. 2014; Jia et al. 2013). Due to the fact that the use of GNT is unavoidable, researchers should find a pharmacological agent that specifically exhibits anti-oxidant and anti-inflammatory effects to counteract its damaging effect on renal tissue.

Ursodeoxycholic acid (UDCA), a hydrophilic bile acid, was used in Chinese medicine to treat non-alcoholic fatty liver (Shi et al. 2012). It was approved by the FDA for treatment of primary biliary cirrhosis (Ikegami and

Matsuzaki 2008). Its hepatocellular protective effect has been studied before, where it has been shown to have anti-oxidant property. In fact, UDCA restores the activities of anti-oxidant mechanisms, superoxide dismutase (SOD) and catalase (CAT), increases levels of reduced glutathione (GSH), reduces the generation of reactive oxygen species (ROS) and activates the nuclear factor E2-related factor-2 (Nrf2), a cellular sensor for oxidative stress (Akbulut et al. 2015; Okada et al. 2008; Rodrigues et al. 1998). Several studies have demonstrated the cytoprotective actions of UDCA on many organ systems. In this regard, Akbulut et al. (2015) demonstrated that UDCA protects hepatocytes from the toxic effect of cyclosporine. In addition, UDCA protects against diabetic renal injury through its anti-oxidant activities (Cao et al. 2016a). UDCA also inhibits bile acid-induced apoptosis on liver tissue in vivo (Rodrigues et al. 1998). Furthermore, UDCA suppresses apoptosis of dopaminergic neurons in an in vitro model of Parkinson's disease (Chun and Low 2012). Other experiments have also demonstrated anti-inflammatory actions for UDCA. Notably, UDCA attenuates the inflammatory response of the inflammatory bowel disease both in vivo and in vitro (Poupon 2012; Ward et al. 2017).

To the best of our knowledge, the effect of UDCA on GNT-induced nephrotoxicity has not been explored yet. Based on the above-mentioned data, we hypothesize that UDCA could ameliorate GNT-induced oxidative stress, inflammation and renal damage. Therefore, we aim to investigate the possible protective effects of UDCA on GNT-induced renal damage in rats.

## Material and methods

### Animals

Adult male Wistar albino rats weighing 180–200 g were obtained from the animal house of the Faculty of Medicine, Assiut University, Assiut, Egypt. They were maintained at  $24 \pm 1$  °C and 12/12 h dark/light cycle. The animals had free access to standard diet and tap water ad libitum. All experimental procedures were approved by the Institutional Animal Care and Use Committee at Faculty of Medicine, Assiut University and animal care followed the guidelines of the National Research Council.

### Drugs and chemicals

Ursodeoxycholic acid (SEDICO, 6th October City, Egypt) was suspended in 0.5% carboxymethyl cellulose. Carboxymethyl cellulose was dosed as 0.5 ml/100 g orally. GNT used was a commercially used ampule (Gramycin® 80/2 ml ampule).

## Experimental design

Twenty-four rats were divided into four groups, with six rats per group. Allocation of animals in their groups was completely random, where rats were numbered from 1 to 24 and divided into groups 1–4 in group orders using a random digit table in a two-digit manner. Animal groups were treated as follows: control group received 0.5% carboxymethyl cellulose for 15 days, GNT-treated group received vehicle and injected with GNT intraperitoneally at a dose of 100 mg/kg/day for 8 days, UDCA-treated group received UDCA orally by gastric tube at a dose of 60 mg/kg/day for 15 consecutive days and UDCA-pretreated group received UDCA in a dose of 60 mg/kg orally once daily for 7 consecutive days, then UDCA co-administered with GNT for 8 consecutive days.

## Sample preparation

Two hours after the last dose of UDCA, rats were anesthetized with ketamine (100 mg/kg) and then, blood samples and kidneys were collected for biochemical and histological examination. Serum was separated by centrifugation at a speed of 4000 rpm for 10 min at 4 °C using a cooling centrifuge (Beckman model L3-50, USA) and stored at –20 °C. Kidney tissues were processed and divided into four parts: the first part was fixed in 10% formalin buffer saline for histopathological and immune-staining and another part was homogenized in ice-cooled phosphate buffer saline using a homogenizer (Potter-Elvehjem rotor-stator homogenizer, USA) to obtain 10% homogenate. Aliquots of the kidney homogenate were stored at 0–4 °C prior to biochemical analysis. The third part was frozen in liquid nitrogen and stored at –80 °C for PCR reaction. The last part was processed for electron microscopy.

## Assessment of renal function parameters

The kidney tissue homogenates were used to determine the kidney function parameters.

## Determination of serum urea

Urea in rat serum was measured according to Fawcett and Scott (1960). We used a kit purchased from Biodiagnostic Co., Giza, Egypt and followed the manufacturer's instructions. Briefly, urea in the samples was hydrolyzed by urease enzyme. The ammonium ions formed are measured by the Berthelot reaction. The blue dye indophenol product reaction absorbs light proportional to initial urea concentration. The absorbance was measured spectrophotometrically at 580 nm.

## Determination of serum creatinine

Creatinine was measured in rat serum as described by Bartels et al. (1972). We used a kit purchased from Biodiagnostic Co., Giza, Egypt and followed the manufacturer's instructions. Briefly, creatinine forms a colored complex with picric acid in an alkaline medium. The absorbance of the samples was measured spectrophotometrically at 510 nm. The density of the color is proportional to the creatinine concentration.

## Determination of serum uric acid

Serum uric acid levels were determined using a uric acid Liquizyme kit (Egyptian Company for Biotechnology, Cairo, Egypt) following the manufacturer's instructions. The assay is based on oxidation of uric acid to allantoin by uricase with production of hydrogen peroxide and carbon dioxide. Peroxide reacts with 4-amino-antipyrine and dichlorohydroxybenzen sulfonate (DCHBs) in the absorbance at 546 nm is proportional to uric acid concentration in the sample.

## Determination of serum albumin

Serum albumin was measured according to Dumas et al. (1997). A kit purchased from the Egyptian Company for Biotechnology, Cairo, Egypt, was used. Briefly, albumin binds to the indicator dye bromocresol green (BCG) in pH 4.1 to form a blue-green-colored complex. The intensity of the blue-green color is directly proportional to the concentration of albumin in the sample. The absorbance was measured spectrophotometrically at 623 nm.

## Determination of urine albumin/creatinine ratio

Urine samples were spun at 4000 rpm to remove cell debris. Urine creatinine was measured according to Jaffe's method. A kit purchased from the Egyptian Company for Biotechnology, Cairo, Egypt, was used. Briefly, creatinine reacts with picric acid under alkaline condition to form a yellow-red complex. The absorbance was measured at 492 nm and it is directly proportional to creatinine in the sample. Urine albumin was measured according to Dumas et al. (1997) using a kit purchased from the Egyptian Company for Biotechnology, Cairo, Egypt. The assay is based on binding of albumin to an indicator dye, bromocresol green, in pH 4.1 to form a green-colored complex. The absorbance was read at 623 nm. The intensity of

the green color is directly proportional to albumin in the sample. The urine albumin/creatinine ratio defines the urine albumin excretion.

### Determination of renal somatic index

Animals were weighed and then sacrificed. Kidneys were immediately removed, washed several times with 0.9% sterile saline solution to remove any blood from the tissue and then blotted with filter papers to absorb excess saline solution. Then, each kidney was weighed. The renal somatic index (RSI) was calculated according to the following equation:  $RSI = (\text{weight of the kidney in gram} / \text{final body weight in gram}) \times 100$ .

### Assessment of oxidative stress biomarkers

The supernatant of the renal tissue homogenates was used to estimate the renal levels of oxidative stress biomarkers.

### Estimation of reduced glutathione activity

Reduced glutathione activity in kidney homogenates was determined using Ellman's reagent according to the method described by Ellman (1959). The assay is based on the reduction of Ellman's reagent [5, 5'-dithio-bis (2-nitrobenzoic acid)] by SH groups to form 1 mol of 2-nitro-5-mercaptobenzoic acid per mole of SH. The nitromercaptobenzoic acid has an intense yellow color and is directly proportional to the GSH concentration. The absorbance was measured spectrophotometrically at 412 nm.

### Estimation of the renal content of malonaldehyde

The renal content of malonaldehyde (MDA), the end product of lipid peroxidation, was estimated according to a previously published method (Mihara and Uchiyama 1978). The principal of the method is that MDA reacts with thiobarbituric acid (TBA) to form a pink color. Briefly, 0.5 ml of tissue homogenate, 3 ml of 1% *O*-phosphoric acid and 1 ml of 0.6% TBA were added in succession to a centrifuge tube. The tubes were incubated in a water bath at 95 °C for 45 min. After cooling to room temperature, 2 ml of *n*-butanol was added to the mixture and vortexed for 1 min. Then, the butanol phase (upper layer) was separated by centrifugation at 2000 rpm for 10 min. The intensity of the red color was measured at 535 and 520 nm.

### Estimation of superoxide dismutase activity

The hepatic SOD activity was estimated according to the method described by Marklund (1985) and depending on the inhibition of pyrogallol autoxidation by SOD. The inhibition is directly proportional to the activity of SOD in the tested sample. In brief, 50  $\mu$ l of tissue homogenate was added to 1 ml of 24 mmol/l pyrogallol in 10 mmol/l HCl and 1 ml of Tris-EDTA buffer (pH 8.6). Changes in the absorbance at 420 nm were recorded for 3 min at 1 min intervals. One unit of SOD activity is defined as the amount of the enzyme causing 50% inhibition of autoxidation of pyrogallol.

### Estimation of renal contents of nitrite/nitrate

Nitrite production, an indicator of nitric oxide (NO) synthesis, was estimated according to the previously described method (Montgomery and Dymock 1961). Briefly, in an acid medium and in the presence of nitrate, the formed nitrous acid diazotizes sulphanilamide and the product are coupled with NEDD (N-(1-naphthyl) ethylenediamine). The resulting azo-day has bright reddish-purple color that can be measured calorimetrically at 540 nm.

### Determination of myeloperoxidase activity

The myeloperoxidase (MPO) activity in the kidney was determined according to the method described by Manktelow and Meyer (1986). MPO activity was assayed by measuring the  $H_2O_2$  released following oxidation of dimethoxybenzidine spectrophotometrically at 460 nm. In this assay, renal homogenate was diluted 1:1 with 0.5% hexadecyl trimethyl ammonium bromide on ice. The homogenate was centrifuged at 4000 rpm for 15 min at 4 °C. The supernatant was transferred to a glass test tube containing 2 ml of chloroform. The tube was allowed to stand for 20 min, then 1 ml of the top aqueous phase was pipetted out and centrifuged at 8000 rpm for 15 min. A total of 200  $\mu$ l supernatant was placed in a glass tube and mixed with 500  $\mu$ l phosphate buffer saline and 600  $\mu$ l of Hanks balanced salt solution containing 0.25% bovine serum albumin. Then, 100  $\mu$ l of 0.125% dimethoxybenzidine and 100  $\mu$ l of 0.05%  $H_2O_2$  were added and the mixture was vortexed for 1 min. The reaction mixture was allowed to stand at room temperature for 15 min. The enzymatic reaction was terminated by addition of 0.5 ml of 1% sodium azide. The released  $H_2O_2$  in the reaction medium after the oxidation of dimethoxybenzidine by MPO was measured spectrophotometrically at 460 nm.



## Real-time PCR

Total RNA was isolated from the tissues using RNA extraction kit according to manufacturer's instructions (GF-1 Total RNA Extraction, Vivantis Technologies, Malaysia). RNA concentration was estimated using SPECTROstar<sup>Nano</sup> spectrometer (BMG Labtech, France) following the manufacturer's instructions. Single-stranded cDNA was synthesized from 1 µg total RNA using cDNA synthesis kit (2-step RT-PCR kit, Vivantis Technologies, Malaysia) following the manufacturer's instructions. Total reaction of 20 µl was performed in real-time PCR plate. Amplification reaction mixture contains 2.5 µl of cDNA, 2 µl of each primer (10 µM), 10 µl SYBR Green master mix (Thermo Scientific, USA) and 3.5 µl of RNA free water. The samples were incubated in the real-time thermocycler (Applied Biosystems StepOne, USA) as per one cycle and for 35 cycles of the following reactions: initial denaturation (95 °C, 3 min), denaturation (95 °C, 30 s), annealing (varies depending on gene, 30 s), extension (72 °C, 40 s) and final extension (72 °C, 5 min). The primers used for NF-κB were 5' TGGGACGACACCTCTACACA-3' (sense) and 5' GGAGCTCATCTCATAGTTGTCC-3' (anti-sense) and for KIM-1 were 5'-GTACACTCACCATG GTAACC-3' (Sense) 5'-AACGCAGCGATTGTGCATCC-3' (anti-sense). B-actin primers were 5'-CCACCATGTACCCA GGCATT-3' (sense) and 5'-ACGCAGCTCAGTAA CAGTCC-3 (anti-sense).

## Immunohistochemistry

Sections at 4 µm thickness prepared from different animal groups were deparaffinized and rehydrated and endogenous peroxidase activity was blocked with 3% H<sub>2</sub>O<sub>2</sub> in methanol. Sections were pre-treated in citrate buffer (pH 6.0) in a microwave. Sections were incubated at room temperature with rabbit polyclonal antibodies specific for the rat targets. The antibodies used were anti-caspase-3 and anti-endothelial nitric oxide synthase (eNOS) antibodies (Thermo Scientific, USA, dilution 1:1000). Then, the tissue sections were rinsed with TBS containing 0.05% Tween 20 twice and incubated with secondary antibody; goat anti-rabbit IgG-HRP conjugate (Vivantis Technologies, Malaysia) at a dilution of 1:5000, for 1 h at 4 °C. After another wash with TBS containing 0.05% Tween 20, the immunoreactivity was developed with 0.05% diaminobenzidine (DAB) and 0.01% H<sub>2</sub>O<sub>2</sub> for 1–3 min and the tissue sections were observed for brown color formation under bright field using a light microscope. Slides were counterstained with hematoxylin. Sections were photographed under a light microscope (Olympus BX50, Tokyo, Japan) and figures were made using CorelDraw software. The percent of area occupied by the immunopositive cell color was measured in four separate microscopic fields in each slide using a digital imaging software program

(ImageJ software). The mean area for each slide was obtained and then, the mean ± SEM was calculated for each group.

## Histological examination

Fixed kidney tissues were dehydrated in ascending grades of ethanol, cleared in xylene, embedded in paraffin and sectioned at a thickness of 5 µm. Sections were stained with hematoxylin and eosin and periodic acid-Schiff (PAS) according to previously described methods (Drury and Wallington 1980). Stained sections were photographed under a light microscope (Leica Q 500 MCO, Germany) and figures were made using CorelDraw software.

Kidney samples for electron microscopy were prepared according to previously described methods (Bozzola 1998). Briefly, samples were immersed in 4% glutaraldehyde in cacodylate buffer for 24 h and then post-fixed in osmium tetroxide in phosphate buffer for 2 h. Semi-thin sections (1 µm) were cut, stained with toluidine blue and examined using a light microscope. Ultrathin sections (500–800 Å) were prepared from selected areas in semi-thin sections, mounted on copper grids and contrasted with uranyl acetate and lead citrate. They were subsequently examined and photographed using a JEOL100 CX Japan transmission electron microscope at 80 kV at the Assiut University Electron Microscopic Unit.

## Statistical analysis

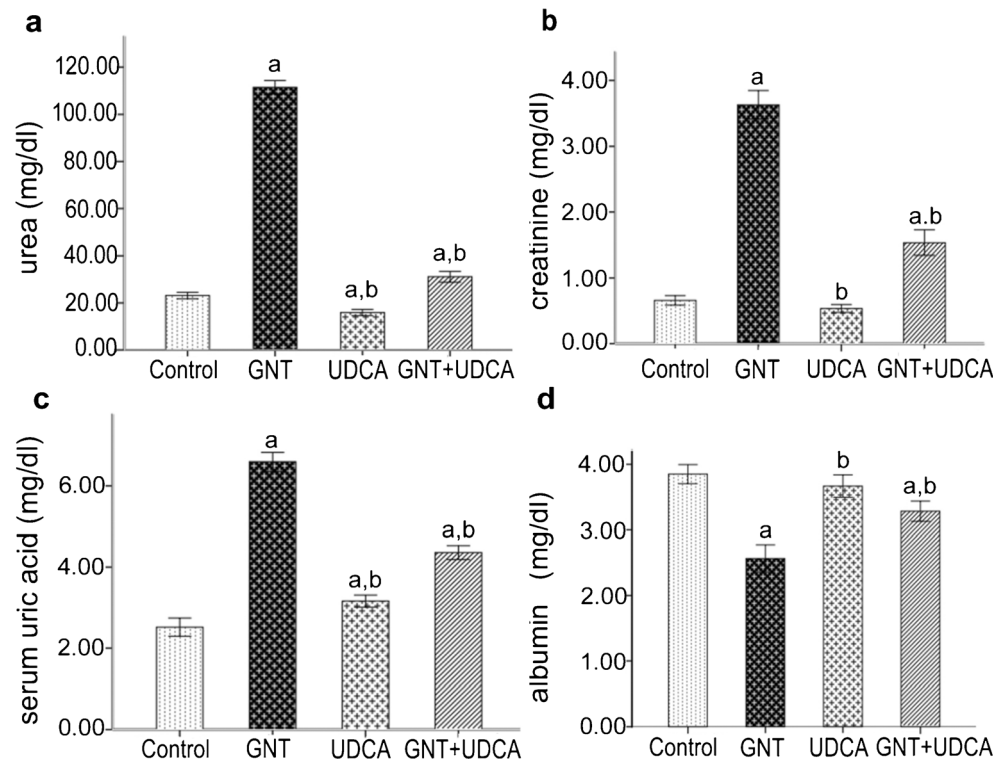
Data are presented as mean ± SE. Statistical analysis of the data was carried out using one-way analysis of variance (ANOVA) followed by Tukey's multiple comparison test for post-hoc analysis. Statistical significance was acceptable to a level of  $p < 0.05$ . Data analysis was accomplished using the Statistical Package for Social Sciences (SPSS) software program (version 20). All measurements were performed in a triplicate manner to keep SE to a minimum as possible.

## Results

### Effect of UDCA on GNT-induced changes in renal function parameters

In order to study the protective effect of UDCA on GNT-induced deterioration of renal function, we pretreated our rats with UDCA once daily for 7 consecutive days then co-administered with GNT intraperitoneally for 8 consecutive days. Our results showed that GNT significantly increased serum levels of urea, whereas pretreatment with UDCA significantly decreased serum levels of urea by a fold of change of  $-0.72$  compared to the GNT-treated group (Fig. 1a and Table 1). Similarly, GNT significantly increased serum creatinine levels, whereas pretreating rats with UDCA significantly

**Fig. 1** Effect of pretreatment with UDCA on gentamycin-induced changes in the serum level of kidney function parameters. Representative graphs of the serum levels of urea (a), creatinine (b), uric acid (c) and albumin (d). Data expressed as mean  $\pm$  SEM ( $n = 6$ ). **a** Significantly different from the normal group at  $p < 0.05$ . **b** Significantly different from the GNT group at  $p < 0.05$



decreased serum creatinine levels by a fold of change of  $-0.58$  compared to GNT-treated rats (Fig. 1b and Table 1). Additionally, GNT significantly increased serum uric acid levels, while administration of UDCA before GNT significantly decreased serum uric acid levels by a fold of change of  $-0.34$  compared to GNT-treated animals (Fig. 1c and Table 1). Moreover, rats treated with GNT showed significantly decreased serum albumin, whereas animals pretreated with UDCA showed a significant increase in serum albumin by a fold of change of  $0.28$  compared to GNT-treated animals (Fig. 1d and Table 1). Furthermore, animals treated with GNT showed a significant increase in urinary excretion of protein, estimated by the urine albumin/creatinine ratio, whereas

UDCA pretreatment significantly decreased urinary excretion of protein by a fold of  $-0.23$  compared to GNT-treated group (Fig. 2a and Table 1).

### Effect of UDCA on GNT-induced kidney injury

The kidney injury molecule-1 (KIM-1) is a transmembrane protein used as a sensitive marker for renal injury by several researchers (Han et al. 2002; Vaidya et al. 2006). We sought to investigate the effect of pretreatment with UDCA on GNT-induced renal expression of KIM-1 at the mRNA levels. We observed that GNT markedly increased KIM-1 mRNA levels, whereas pretreatment with UDCA

**Table 1** Effect of UDCA on gentamycin-induced changes in kidney function parameters

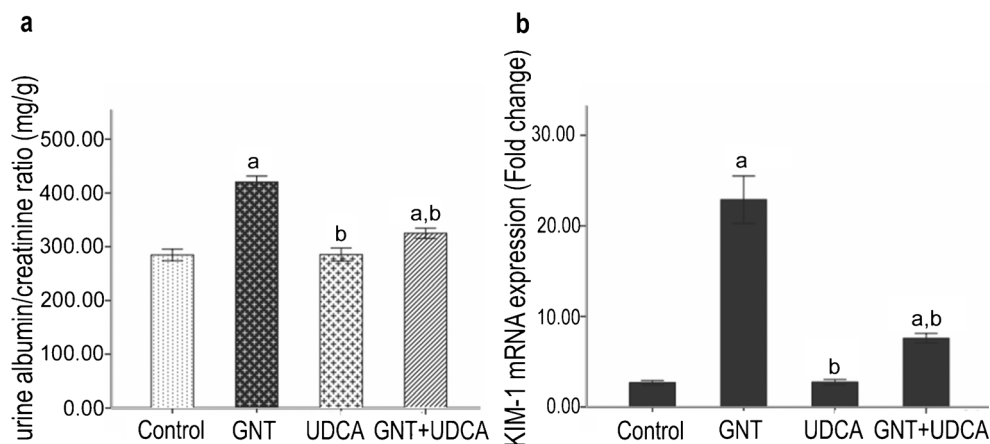
Parameters	Normal group	GNT-treated group	UDCA group	GNT + UDCA
Urea (mg/dl)	23.16 $\pm$ 0.541	111.54 $\pm$ 1.071 <sup>a</sup>	15.89 $\pm$ 0.513 <sup>a,b</sup>	31.12 $\pm$ 0.884 <sup>a,b</sup>
Creatinine (mg/dl)	0.66 $\pm$ 0.028	3.63 $\pm$ 0.085 <sup>a</sup>	0.54 $\pm$ 0.023 <sup>a,b</sup>	1.53 $\pm$ 0.075 <sup>a,b</sup>
Uric acid (mg/dl)	2.52 $\pm$ 0.087	6.59 $\pm$ 0.090 <sup>a</sup>	3.16 $\pm$ 0.059 <sup>a,b</sup>	4.36 $\pm$ 0.067 <sup>a,b</sup>
Albumin (g/dl)	3.85 $\pm$ 0.056	2.57 $\pm$ 0.080 <sup>a</sup>	3.67 $\pm$ 0.067 <sup>b</sup>	3.28 $\pm$ 0.060 <sup>a,b</sup>
Urine albumin/creatinine ratio (mg/g)	284.35 $\pm$ 4.185	420.80 $\pm$ 4.228 <sup>a</sup>	285.38 $\pm$ 4.765 <sup>b</sup>	324.97 $\pm$ 3.745 <sup>a,b</sup>

Data are expressed as mean  $\pm$  SEM ( $n = 6$ ) and analyzed by one-way ANOVA followed by post-hoc Tukey's test GNT, gentamicin; UDCA, ursodeoxycholic acid

<sup>a</sup> Significantly different from the normal group at  $p < 0.05$

<sup>b</sup> Significantly different from the GNT group at  $p < 0.05$

**Fig. 2** Effect of pretreatment with UDCA on gentamycin-induced changes in urine albumin/creatinine ratio (a) and KIM-1 mRNA levels (b). Data expressed as mean ± SEM (*n* = 6). **a** Significantly different from the normal group at *p* < 0.05. **b** Significantly different from the GNT group at *p* < 0.05



significantly decreased KIM-1 mRNA levels compared to GNT-treated animals (Fig. 2b).

**Effect of UDCA on GNT-induced oxidative stress**

In order to investigate whether UDCA alleviates GNT-induced oxidative stress, we investigated the renal tissue GSH activities in response to pretreatment with UDCA. We observed that renal GSH activities were significantly decreased in GNT-treated rats by a fold of -0.52 compared to the control rats. In contrast, pretreatment with UDCA significantly increased the renal GSH activities by a fold of 0.31 compared to the GNT alone-treated rats (Fig. 3a and Table 2).

We also examined the effect of pretreatment with UDCA on the activity of SOD enzyme in renal tissue. We observed a significant decrease in renal SOD activities, whereas pretreatment with UDCA significantly increased the activity of SOD in renal tissue by a fold of 1.3 compared to the GNT alone-treated animals (Fig. 3b and Table 2).

**Effect of UDCA on GNT-induced lipid peroxidation and nitric oxide production**

In order to test whether UDCA alleviates lipid peroxidation induced by GNT, we estimated the renal tissue levels of MDA, the end product of lipid peroxidation. We observed

**Fig. 3** Effect of pretreatment with UDCA on gentamycin-induced alterations in renal oxido-nitrosative stress biomarkers. Representative graphs of GSH (a) and SOD (b) activities and MDA (c) and NOx (d) levels. Data expressed as mean ± SEM (*n* = 6). **a** Significantly different from the normal group at *p* < 0.05. **b** Significantly different from the GNT group at *p* < 0.05

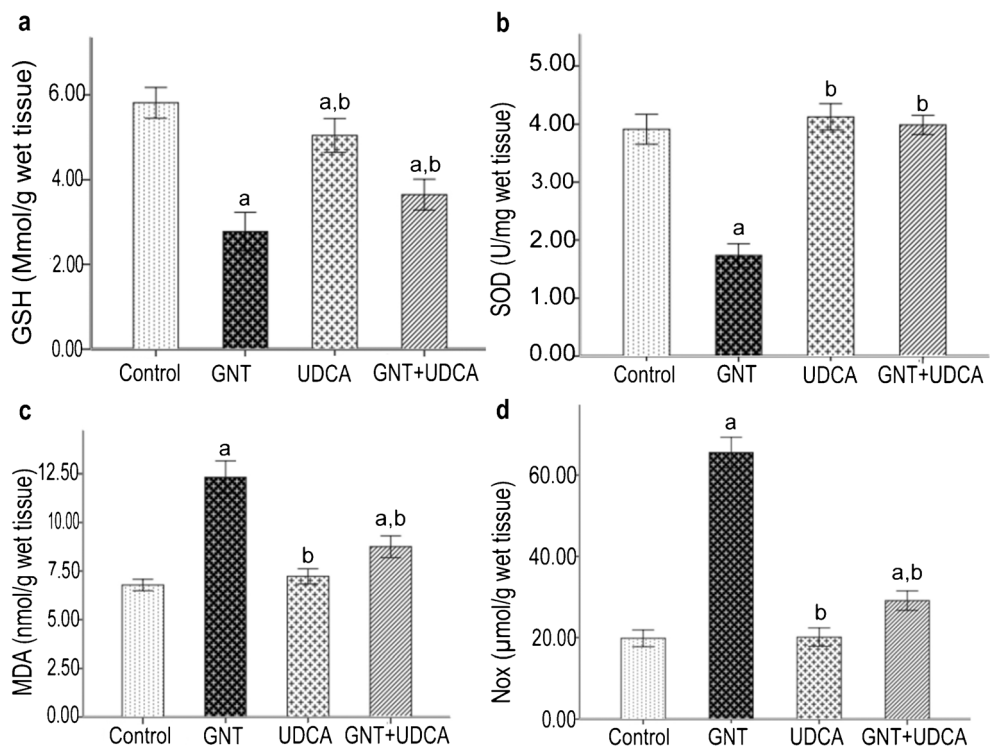


**Table 2** Effect of UDCA on gentamycin-induced changes in renal oxido-nitrosative stress biomarkers

Parameters	Normal group	GNT group	UDCA group	GNT + UDCA
GSH ( $\mu\text{mol/g}$ wet tissue)	$5.82 \pm 0.139$	$2.78 \pm 0.177^a$	$5.95 \pm 0.156^b$	$3.65 \pm 0.142^{a,b}$
SOD (U/mg wet tissue)	$3.91 \pm 0.101$	$1.73 \pm 0.078^a$	$4.13 \pm 0.087^b$	$3.99 \pm 0.064^b$
MDA (nmol/ g wet tissue)	$6.78 \pm 0.115$	$12.33 \pm 0.322^a$	$7.22 \pm 0.151^b$	$8.77 \pm 0.218^{a,b}$
NOx ( $\mu\text{mol/g}$ wet tissue)	$19.815 \pm 0.804$	$65.46 \pm 1.460^a$	$20.09 \pm 0.880^b$	$29.09 \pm 0.933^{a,b}$

Data are expressed as mean  $\pm$  SEM ( $n = 6$ ) and analyzed by one-way ANOVA followed by post-hoc Tukey's test *GSH*, reduced glutathione; *SOD*, superoxide dismutase; *MDA*, malondialdehyde; *NOx*, nitric oxide end products; *GNT*, gentamicin; *UDCA*, ursodeoxycholic acid

<sup>a</sup>Significantly different from the normal group at  $p < 0.05$

<sup>b</sup>Significantly different from the GNT group at  $p < 0.05$

that GNT injection significantly increased renal levels of MDA compared to control animals, whereas renal MDA levels significantly decreased in response to pretreatment with UDCA by a fold of  $-0.29$  compared to rats treated with GNT alone (Fig. 3c and Table 2).

A large body of evidence has linked oxidative stress with NO production (Araujo and Welch 2006; Ikari et al. 2005; Ou et al. 2010). Therefore, we investigated renal nitric oxide production as indicated by renal tissue levels of nitric oxide end products (NOx), nitrite/nitrate, in response to pretreatment with UDCA. We observed that GNT injection significantly increased the renal NOx levels compared to control animals. Whereas, pretreatment with UDCA significantly decreased the renal levels of NOx by a fold of  $-0.56$  compared to GNT-treated rats (Fig. 3d and Table 2).

### Effect of UDCA on GNT-induced alteration in renal MPO activities, RSI and NF- $\kappa$ B mRNA renal levels

In order to test whether pretreatment with UDCA ameliorates GNT-induced increased neutrophil infiltration in the renal tissue, we tested the renal myeloperoxidase (MPO) activities, indicative of neutrophil infiltration. We observed a significant increase in renal MPO activities in animals injected with GNT compared to the control animal. Whereas, a significant decrease in renal MPO activities was observed in rats pretreated with UDCA by a fold of  $-0.33$  compared to rats treated with GNT alone (Fig. 4a and Table 3). Additionally, we determined the RSI, which is kidneys' weights normalized as percentage of total body weight ( $100 \times (\text{kidneys' weights}) / \text{total body weight}$ ), in response to UDCA pretreatment. We observed that

**Fig. 4** Effect of pretreatment with UDCA on gentamycin-induced changes in renal MPO activity (a), RSI (b) and NF- $\kappa$ B mRNA levels (c). Data expressed as mean  $\pm$  SEM ( $n = 6$ ). **a** Significantly different from the normal group at  $p < 0.05$ . **b** Significantly different from the GNT group at  $p < 0.05$

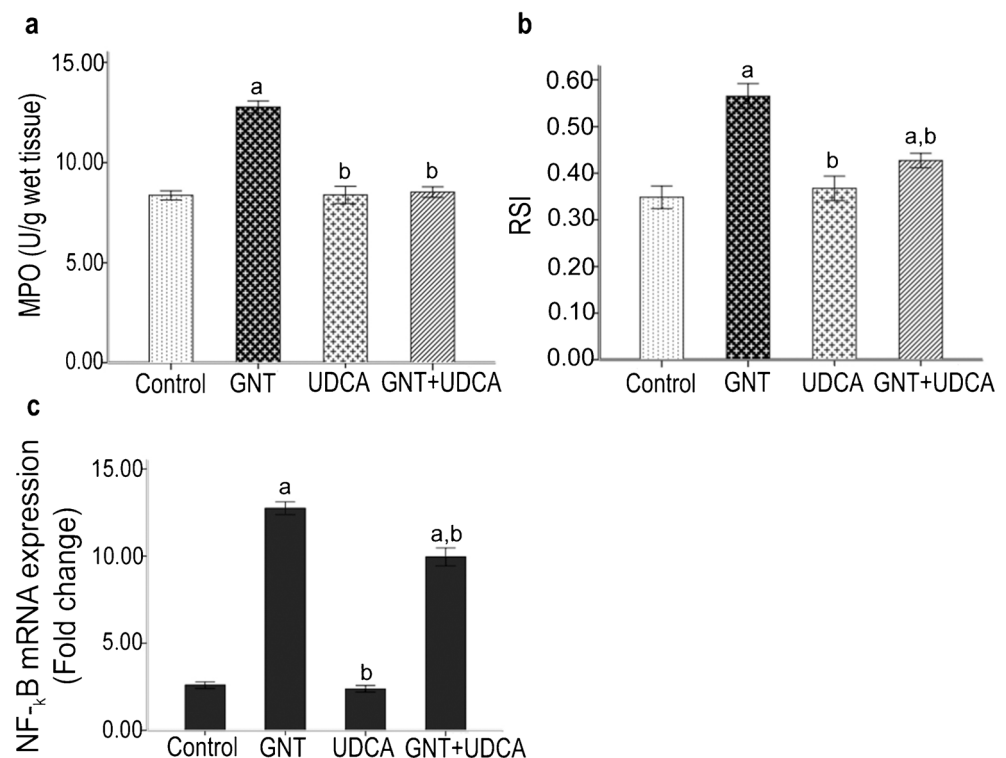




**Table 3** Effect of UDCA on gentamycin-induced changes in MPO and RSI in renal tissue

Parameters	Normal group	GNT group	UDCA group	GNT + UDCA
MPO (U/g wet tissue)	8.36 ± 0.089	12.79 ± 0.116 <sup>a</sup>	8.38 ± 0.168 <sup>b</sup>	8.52 ± 0.103 <sup>b</sup>
RSI	0.35 ± 0.009	0.57 ± 0.010 <sup>a</sup>	0.37 ± 0.010 <sup>b</sup>	0.43 ± 0.006 <sup>a,b</sup>

Data are expressed as mean ± SEM ( $n = 6$ ) analyzed by one-way ANOVA followed by post-hoc Tukey's test  
*MPO*, myeloperoxidase; *RSI*, renal somatic index; *GNT*, gentamicin; *UDCA*, ursodeoxycholic acid

<sup>a</sup> Significantly different from the normal group at  $p < 0.05$

<sup>b</sup> Significantly different from the GNT group at  $p < 0.05$

treatment with GNT alone increased RSI by a fold of 0.63 compared to normal rats. However, pretreatment with UDCA significantly decreased RSI by a fold of  $-0.25$  compared to GNT alone-treated rats (Fig. 4b and Table 3). Furthermore, we evaluated the renal expression of nuclear factor kappa B (NF- $\kappa$ B), the key factor for renal inflammation, at the mRNA level in response to UDCA pretreatment. We observed that GNT treatment significantly increased the relative expression of NF- $\kappa$ B mRNA in renal tissues compared to control animals (Fig. 4c). In contrast, pretreatment animals with UDCA showed a significant reduction in renal mRNA expression of NF- $\kappa$ B (Fig. 4c).

### Effect of UDCA on GNT-induced alteration in renal expression of endothelial nitric oxide synthase

In order to investigate the effect of UDCA on GNT-induced change in eNOS protein expression, we employed the immunohistochemical technique. In control rats, eNOS protein expression was observed in renal glomeruli (Fig. 5a, arrow heads) as well as tubules (Fig. 5a, arrows). In contrast, kidney tissue from rats treated with GNT showed a decrease in eNOS protein expression in renal glomeruli (Fig. 5b, arrow heads) and tubules (Fig. 5b, arrows) compared to control rats. On the other hand, treating rats with UDCA before administration of GNT and co-administration of UDCA and GNT to the end of the experiment increased expression of eNOS in renal glomeruli (Fig. 5d, arrowheads) and tubules (Fig. 5d, arrows) compared to GNT only-treated rats. Surprisingly, eNOS protein expression was intensely expressed both in glomeruli (Fig. 5c, arrow heads) and renal tubular cells (Fig. 5c, arrows) in UDCA-treated group compared to the control animals. Quantitative analysis of eNOS protein expression showed a significant reduction in the expression of eNOS in rats treated with GNT compared to the control animals, whereas pretreatment with UDCA significantly increased the expression of eNOS compared to the GNT-treated animals (Fig. 5e and Table 4).

### Effect of UDCA on GNT-induced alteration in renal expression of caspase-3

To explore whether pretreatment with UDCA has an effect on GNT-induced apoptosis, we evaluated the expression of the

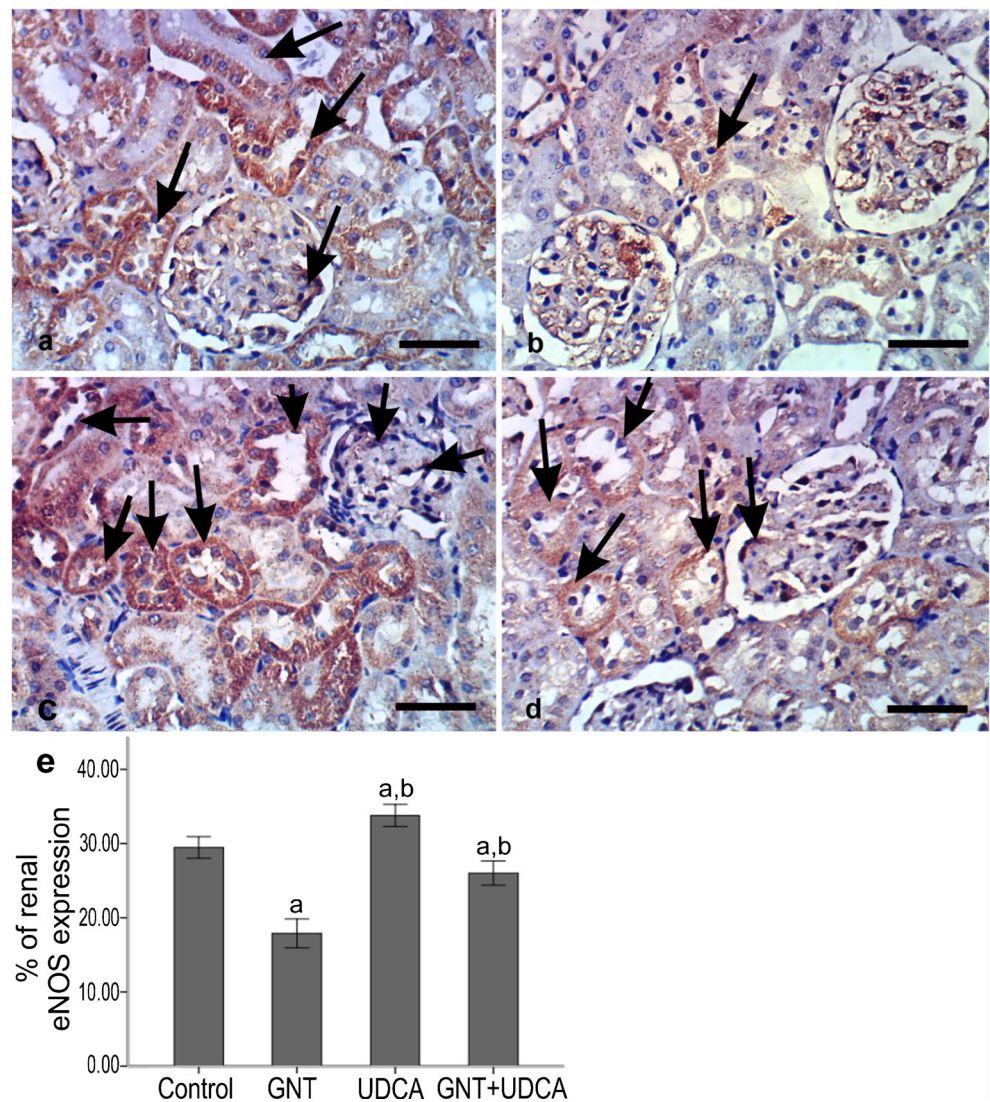
apoptotic parameter caspase-3 in renal tissues using the immunohistochemistry technique. In control rats, the expression of caspase-3 was minimal in both renal tubular cells and glomeruli (Fig. 6a, arrows). On the other hand, injection of GNT leads to a marked increase in the expression of caspase-3 in renal tubular cells and to a lesser extent in renal glomeruli compared to control animals (Fig. 6b, arrow). However, pretreatment with UDCA significantly decreased caspase-3 in the renal tubules and glomeruli (Fig. 6d, arrows) compared to animals treated with GNT alone. Like control rats, administration of UDCA alone induced minimal changes in caspase-3 expression (Fig. 6c). Quantitative analysis of caspase-3 expression by immunohistochemistry showed a significant increase in the expression of caspase-3 in rats treated with GNT compared to the control animals. However, pretreatment with UDCA significantly reduced the expression of caspase-3 compared to the GNT-treated animals (Fig. 6e and Table 4).

### Histological analysis

Histological examination of sections from the renal cortex of control animals as well as rats treated with UDCA only showed that the cortex is crowded with renal corpuscles and tubules of the nephrons with minimal interstitial spaces that show minimal cellular infiltration (Fig. 7a,c, arrows). In contrast, a marked increase in cellular infiltrations in the renal interstitium was observed after injection of animals with GNT (Fig. 7b, arrows). On the other hand, pretreatment with UDCA markedly decreased the cellular infiltration in the renal interstitium compared to GNT-treated animals (Fig. 7d, arrows).

At high magnification, sections from the renal cortex of control rats as well as UDCA-treated animals showed that the renal corpuscle is composed of a glomerular tuft of capillaries (Fig. 8a,c) surrounded by Bowman's capsule with a space, urinary (Fig. 8a,c, stars), separating the parietal layer (Fig. 8a,c, arrow heads) from the visceral layer that adhered to the capillary tuft. Surrounding the renal corpuscles are the proximal convoluted tubules lined by high cuboidal cells with dense eosinophilic cytoplasm and narrow lumens to which the brush border microvilli extend (Fig. 8a,c, arrows) and the distal convoluted tubules lined by low cuboidal cells and have wider lumen (Fig. 8a,c, double-headed arrow). Animals

**Fig. 5** Immunohistochemical localization of eNOS in renal tissues. Representative section from control (**a**), GNT (**b**), UDCA (**c**) and UDCA-pretreated animals (**d**). **a** Expression of eNOS in glomeruli and renal tubules of control animals (arrows in **a**). **b** Shows decreased eNOS immunostaining in GNT-treated rats. Arrows in **c** show intense eNOS immunostaining in the glomeruli and renal tubular cells of rats treated by UDCA. UDCA treatment before gentamycin reversed the reduction of eNOS expression caused by GNT treatment (**d**). Scale bars = 50  $\mu$ m. **e** Quantitative analysis of eNOS expression in renal tissues. Data expressed as mean  $\pm$  SEM ( $n = 6$ ). **a** Significantly different from the normal group at  $p < 0.05$ . **b** Significantly different from the GNT group at  $p < 0.05$



treated with GNT demonstrated foci of glomerular shrinkage with widening of the urinary spaces (Fig. 8b, star). Additionally, renal tubules showed structural changes ranging from cytoplasmic vacuolations (Fig. 8b, short arrows), cellular desquamation (Fig. 8b, arrow heads), to total loss of tubular architecture (Fig. 8b, long arrows). In contrast, kidney sections from animals pretreated with UDCA showed a retained glomerular structure with normally appeared urinary spaces (Fig. 8d, star) and mild cytoplasmic vacuolation of renal tubular cells (Fig. 8d, arrows).

In order to examine the brush border of the renal tubular cells and their basement membranes, we stained kidney sections with PAS. In control and UDCA-treated rats, staining reactions were observed in the brush border of proximal convoluted tubular cells (Fig. 9a,c, arrow heads) and their continuous basement membrane (Fig. 9a,c, arrows). In contrast, GNT-treated animals showed foci with loss of the brush border of the proximal convoluted tubules (Fig. 9b, arrow heads)

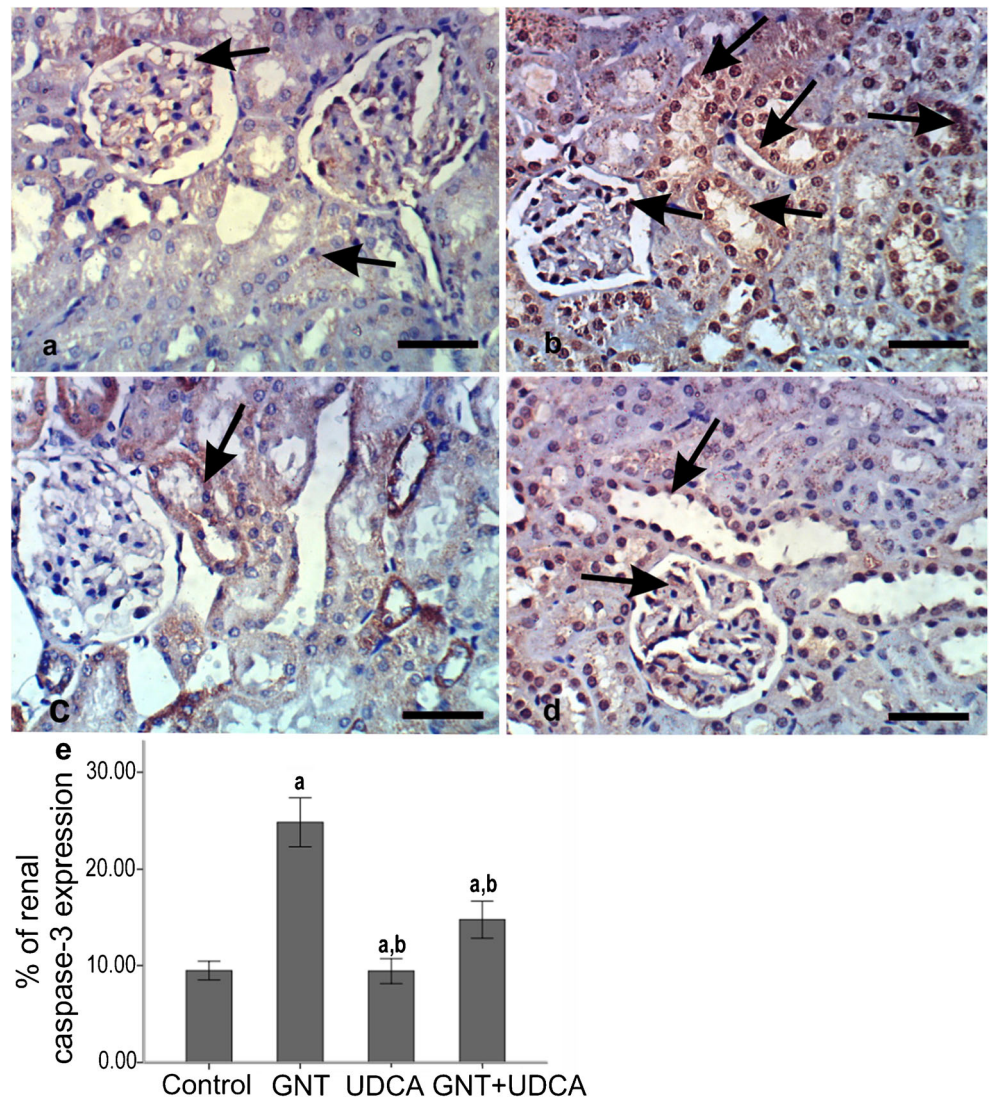
and discontinuous basement membranes (Fig. 9b, arrows). However, animals pretreated with UDCA showed proximal tubules with preserved brush borders (Fig. 9d, arrow heads) and continuous basement membranes (Fig. 9d, arrows).

Additionally, we explored the renal medulla for the presence of casts in PAS-stained kidney sections. In control and UDCA-treated animals, the medulla contains distal and collecting tubules that are lined by cuboidal cells (Fig. 10a,c, arrows) and thin segments of Loop of Henle lined by squamous cells (Fig. 10a,c, arrow heads). The lumens of these tubules appear empty. In contrast, GNT-treated animals showed renal tubules obliterated by PAS-positive hyaline casts (Fig. 10b, arrows). Whereas, animals pretreated with UDCA demonstrated few renal tubules with PAS-positive hyaline casts (Fig. 10d, arrows).

Electron microscopic examination of the renal cortex of control group demonstrated the presence of distinguishable renal corpuscles. They consisted of glomerular capillaries that



**Fig. 6** Immunohistochemical localization of caspase-3 expression in renal tissues. Caspase-3 was predominantly expressed in renal tubular cells. Representative micrographs of sections from control (a), GNT (b), UDCA (c) and UDCA-pretreated animals (d). **a** Renal tissues from control rats show minimal caspase-3 expression. GNT injection increases caspase-3 expression in renal tissue (arrow in **b**). **c** Shows minimal caspase-3 expression in rats treated with UDCA only. Pretreatment with UDCA decreased GNT-induced increase in caspase-3 expression in renal tissues (arrow in **d**). Scale bars = 50  $\mu$ m. **e** Quantitative analysis of caspase-3 expression in renal tissues. Data expressed as mean  $\pm$  SEM ( $n = 6$ ). **a** Significantly different from the normal group at  $p < 0.05$ . **b** Significantly different from the GNT group at  $p < 0.05$



were lined by fenestrated endothelium. Podocytes had euchromatic nuclei and foot processes resting on the surface of the renal glomerular basement membrane (Fig. 11a). This picture of the blood renal filtration barrier was similarly observed in UDCA only-treated group (Fig. 11c). After treatment with GNT, disruption of the blood renal filtration barrier was illustrated by ill-defined endothelial fenestrations, distorted foot processes of podocytes, unapparent filtration slits and an

irregularly thickened basement membrane (Fig. 11b). Additionally, we noticed deposition of the hyaline material in the mesangium (Fig. 11b). Pretreated group with UDCA showed well-defined endothelial fenestrations, normally looked foot processes of podocytes and uniform thickness of the basement membrane (Fig. 11d).

The cells lining the PCT of the control group appeared with euchromatic nuclei and prominent nucleoli. Apical

**Table 4** Effect of the administration of UDCA on eNOS and caspase-3 expression against GNT-induced renal injury in rats

% of protein expression	Normal group	GNT group	UDCA group	GNT + UDCA
eNOS	29.48 $\pm$ 0.456	17.89 $\pm$ 0.609 <sup>a</sup>	33.77 $\pm$ 0.472 <sup>a,b</sup>	26.03 $\pm$ 0.514 <sup>a,b</sup>
Caspase-3	9.48 $\pm$ 0.305	24.83 $\pm$ 0.797 <sup>a</sup>	9.42 $\pm$ 0.407 <sup>a,b</sup>	14.76 $\pm$ 0.609 <sup>a,b</sup>

Data are expressed as mean  $\pm$  SEM ( $n = 6$ ) analyzed by one-way ANOVA followed by post-hoc Tukey’s test eNOS, endothelial nitric oxide synthase

<sup>a</sup> Significantly different from the normal group at  $p < 0.05$

<sup>b</sup> Significantly different from the GNT group at  $p < 0.05$



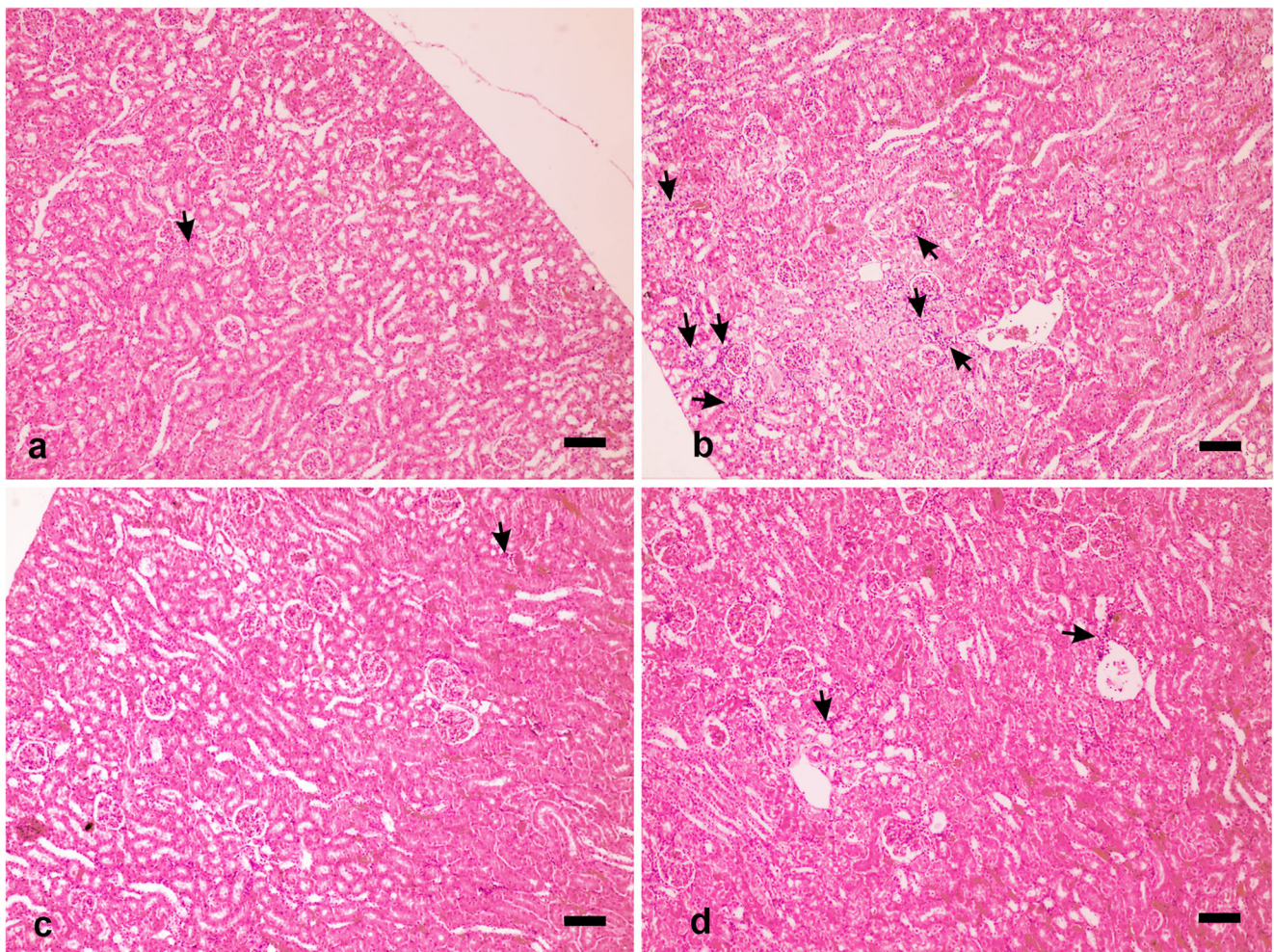


**Fig. 7** Photomicrographs of kidney sections stained with hematoxylin and eosin. **a** Representative section from the kidney from control rats shows minimal cellular infiltration (arrow). **b** A kidney section from GNT-treated rats shows cellular infiltration (arrows) in the renal

interstitium. **c** A kidney section from UDCA-treated rats. **d** A kidney section from rats pretreated with UDCA shows decreased inflammatory cell infiltrations (arrows). Scale bar = 100  $\mu$ m

cell membrane showed well-developed microvilli, while the basal cell membrane was modified in the form of infoldings housing elongated mitochondria. The tubular basement membrane appeared regular and uniform (Fig. 12a). GNT treatment induced ultrastructural changes in the form of ill-defined microvilli at the apical cell border, cytoplasmic vacuoles, either swollen mitochondria or cristae disintegration, accumulation of lysosomes and myeloid bodies and thickening of the basement membrane (Fig. 12b). A remarkable feature of this group was the presence of active fibroblasts in the renal interstitium demonstrating dilated cisternae of rough endoplasmic reticulum (Fig. 12b). In UDCA only-treated rats, cells of the proximal convoluted tubules appeared with more or less normal ultrastructure features (Fig. 12c). Most of the PCT from UDCA-pretreated animals showed reappearance of apical microvilli, with normal thickness of the tubular basement membrane and healthy mitochondrial profiles in spite of persistence of some swollen ones (Fig. 12d).

## Discussion

Previous reports have pointed out to GNT-associated nephrotoxicity both in human and animals (Abdel-Raheem et al. 2009; Appel 1990; Morsy et al. 2014; Sahu et al. 2014b). In this study, we demonstrated for the first time that UDCA could attenuate GNT-induced nephrotoxicity in rats. In our experiments, we showed that UDCA reversed the adverse effect of GNT on kidney function parameters namely, serum urea, creatinine, uric acid, urine albumin and KIM-1 (Figs. 1, 2 and Table 1). UDCA also antagonized the effect of GNT on renal levels of MDA, GSH, SOD and nitric oxide end products NOx (Fig. 3 and Table 2) and endothelial nitric oxide synthase (eNOS) (Fig. 5 and Table 4). In addition, UDCA counteracts GNT-induced changes on the renal levels of MPO and the expression of NF- $\kappa$ B (Fig. 4 and Table 3). Furthermore, UDCA pretreatment decreased the expression of the apoptotic marker, caspase-3 (Fig. 6 and Table 4). Finally, UDCA improved the structural changes in the renal glomeruli and



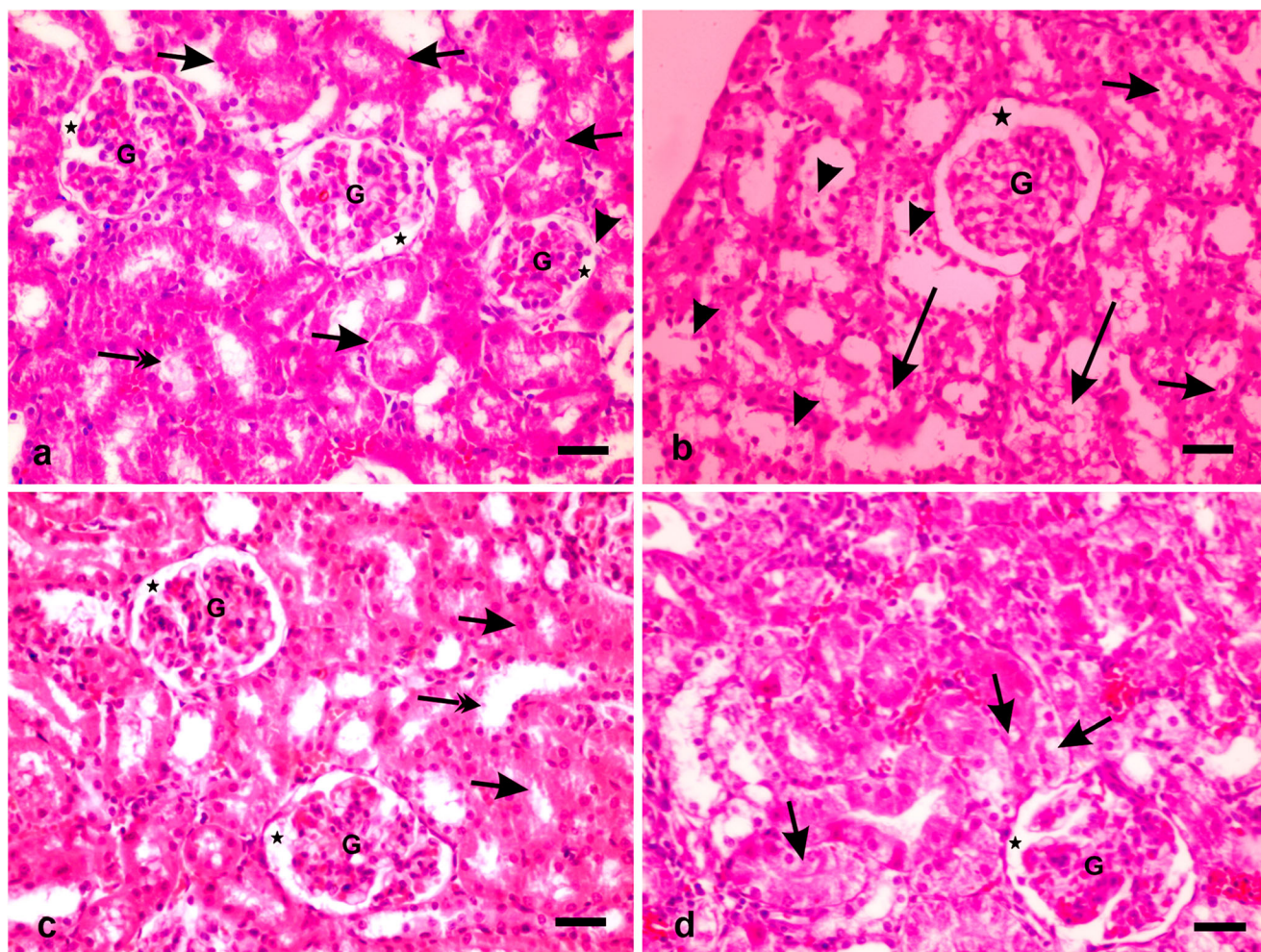


**Fig. 8** Higher magnification photomicrographs of kidney sections stained with hematoxylin and eosin. **a** A kidney section from control rats. **b** A kidney section from rats treated with GNT showing glomerular atrophy (G) with widening of urinary space (star), cytoplasmic vacuolation of tubular cells (short arrows), desquamation of tubular

epithelial cells (arrow heads) and loss of the tubular architecture (long arrows). **c** A kidney section from animals treated with UDCA only. **d** A kidney section from rats pretreated with UDCA shows normal appeared glomeruli and mild cytoplasmic vacuolation of the renal tubules (arrows). Scale bar = 30  $\mu$ m

tubules induced by GNT (Figs. 7–12). Together, it is likely that UDCA exerts its renoprotective effects through its antioxidative, anti-inflammatory and anti-apoptotic properties.

This study in rats shows that administration of GNT produces a significant increase in the RSI, the percentage of the kidney weight to the total body weight, compared to the normal rats (Fig. 4b). The increase in RSI is due to increase in kidney weight caused by inflammation and edema of renal tissues, which are the consequences of the acute tubular damage caused by GNT injection (Erdem et al. 2000), whereas pretreatment of animals with UDCA decreased the RSI compared to the GNT-treated rats. This observation could be attributed to the anti-inflammatory effect of UDCA as reported by Buryova et al. (2013).

In the present study, we showed that GNT markedly elevated serum creatinine and blood urea levels (Fig. 1a,b). This marked elevation of renal function markers is an indication of significant renal impairment (Atici et al. 2005; Schrier et al.

2004). Previous reports have associated the elevation of serum creatinine and blood urea with glomerular damage and decreased glomerular filtration rate (GFR) (Baum et al. 1975; Laurent et al. 1990). In accordance with these observations, our ultrastructural data showed that GNT induced alteration in the filtration barrier as well as increased deposition of the mesangial matrix (Fig. 11b,b). Additionally, we showed luminal casts obliterating the tubular lumens in kidney sections from GNT-treated animals (Fig. 10b). These obliterating casts were likely caused by shedded brush borders and desquamated tubular cells and had been associated with reduction of GFR (Hosaka et al. 2004). In contrast, UDCA-pretreated animals showed significant reduction in serum urea and creatinine. Moreover, pretreatment with UDCA decreased GNT-induced renal glomerular and tubular changes (Figs. 8d, 9d, 11d, and 12d). Furthermore, UDCA pretreatment decreased accumulation of luminal casts in medullary tubules (Fig. 10d). Therefore,



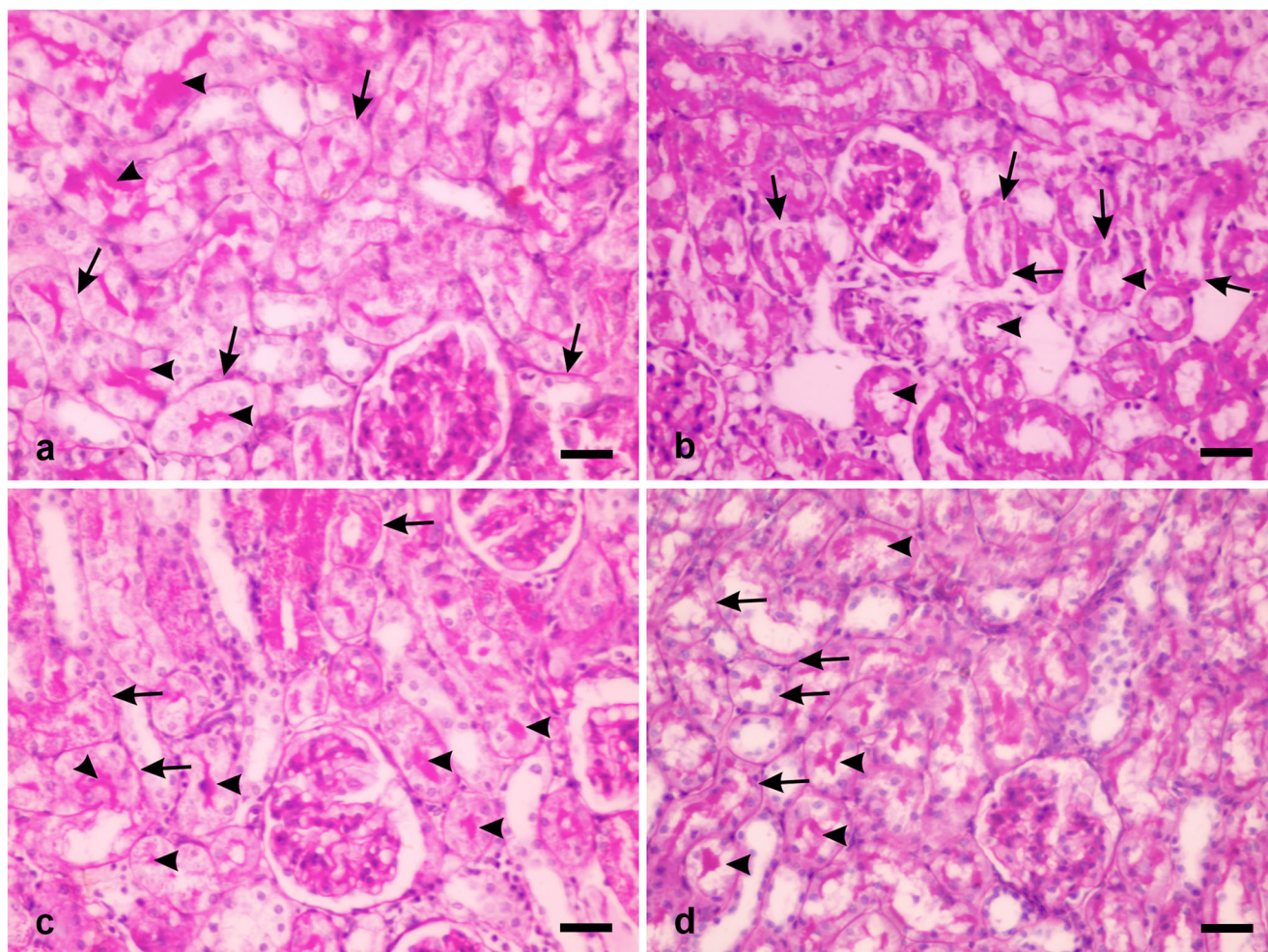


**Fig. 9** Representative micrographs of periodic acid-Schiff-stained renal cortical sections. **a** A section from control animal (arrow heads point to the brush border and arrows point to the basement membrane). **b** A kidney section from GNT-treated animal showing loss of brush border (arrow heads) and basement membrane breakdown (arrows). **c** A kidney

section from UDCA only-treated rats. **d** A kidney section from animals pretreated with UDCA showing renal tubules with brush border at the apices of their cells (arrowheads) and rests on the continuous basement membrane (arrows). Scale bar = 30  $\mu$ m

it is likely that pretreatment with UDCA restored renal function through improvement of GFR due to decrease of the GNT-induced glomerular and tubular changes and formation of casts.

Another important marker of impaired kidney function is increased excretion of albumin in urine (albuminuria). Normally, the glomerular barrier retains albumin in the blood and small fractions that pass the barrier are reabsorbed via megalin, a membrane glycoprotein, through receptors mediated by endocytosis (Gorriz and Martinez-Castelao 2012; Sun et al. 2017). Interestingly, Nagai et al. (2006) demonstrated that GNT binds to the proximal tubular brush border membrane at megalin receptors. More importantly, GNT competitively inhibited reuptake of bovine serum albumin by megalin receptors in the apical membrane of proximal tubular cells (Cui et al. 1996). Furthermore, GNT has been shown increasing the glomerular permeability to albumin (de-Barros-e-Silva et al. 1992). Here, we demonstrated that GNT increased urinary

excretion of albumin (Fig. 2a). This finding was associated with changes in the blood renal filtration barrier at the ultra-structure level (Fig. 11b). However, pretreatment with UDCA significantly decreased urinary excretion of albumin (Fig. 2a). Additionally, pretreatment with UDCA prevented GNT-induced filtration barrier changes (Fig. 11d). This protective role of UDCA could be attributed to restoration of the glomerular barrier functions through reduction of podocyte apoptosis by downregulation of caspase-3 and caspase 12 as shown by Cao and colleagues in a murine model of diabetic nephropathy (Cao et al. 2016b). Another possibility is that UDCA could inhibit the interaction of GNT with megalin. This inhibition facilitates reabsorption of albumin by proximal tubular cells. This role of UDCA needs to be further examined.

An important biomarker for kidney injury is the KIM-1. It is a transmembrane glycoprotein expressed at high levels predominantly on the apical membrane of the proximal tubular



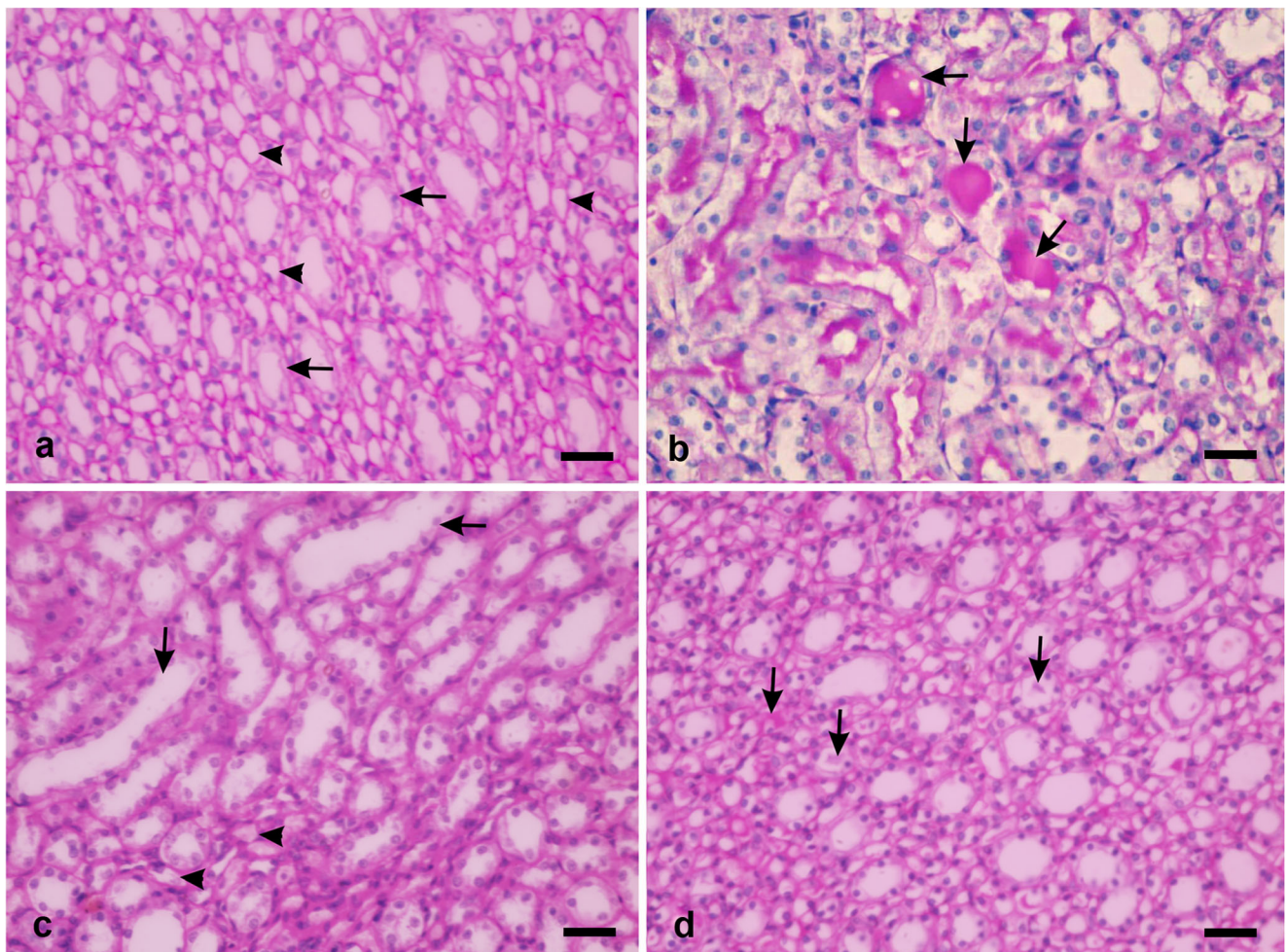


**Fig. 10** Representative micrographs of periodic acid-Schiff-stained kidney sections showing part of the medulla. **a** Shows renal sections from control animals. **b** Shows PAS-positive hyaline casts obliterating renal

tubular lumina (arrows). **c** Shows kidney section from UDCA-treated animals. **d** A kidney section from UDCA-pretreated animals with a few hyaline casts (arrows). Scale bar = 30  $\mu$ m

cells after renal injury and not detectable in normal kidney tissues (Luo et al. 2016). In accordance with previous reports, we found increased expression of renal KIM-1 mRNA levels of rats treated with GNT (Chen et al. 2017; Luo et al. 2016). In contrast, we observed reduction of renal KIM-1 mRNA levels of rats pretreated with UDCA. This observation is in accord with our histological findings at the tubular levels (Fig. 8d) and supports the idea that pretreatment with UDCA reduces GNT-induced renal injury.

It is well-known that free radicals play an important role in GNT-induced nephrotoxicity (Lee et al. 2012; Otunctemur et al. 2013; Shin et al. 2014). Free radicals induce tissue damage by several mechanisms including degradation of membrane phospholipids through lipid peroxidation and protein modification (Edson and Terrell 1999; Priuska and Schacht 1995; Yanagida et al. 2004). In accordance with Kalayarasan et al.'s (2009) observation, we demonstrated that GNT significantly increased in tissue levels of MDA, indicative of increased lipid peroxidation (Fig. 3c). However, pretreatment

with UDCA greatly reduced the GNT-induced elevation of MDA levels (Fig. 3c). Moreover, we showed that the SOD enzyme activity has been significantly reduced in GNT-treated rats (Fig. 3b). This reduction in renal SOD activity could be attributed to the increased production of superoxide anions by GNT. In contrast, pretreatment of rats with UDCA significantly increased the SOD activity (Fig. 3b). Furthermore, we (Fig. 3a) and others (Adil et al. 2016; Jose et al. 2017) have demonstrated that GNT treatment significantly reduced GSH activity. However, pretreatment with UDCA significantly increased the GSH activity (Fig. 3a). These observations are in line with previous reports (Chen et al. 2011; Osorio et al. 2012) and support the idea that pretreatment of rats with UDCA reduced GNT-induced oxidative stress. This effect could be attributed to the direct free radical scavenging activity of UDCA as suggested by Lapenna et al. (2002) and/or its role in upregulation of antioxidant gene expression as reported by Mitsuyoshi et al. (1999).



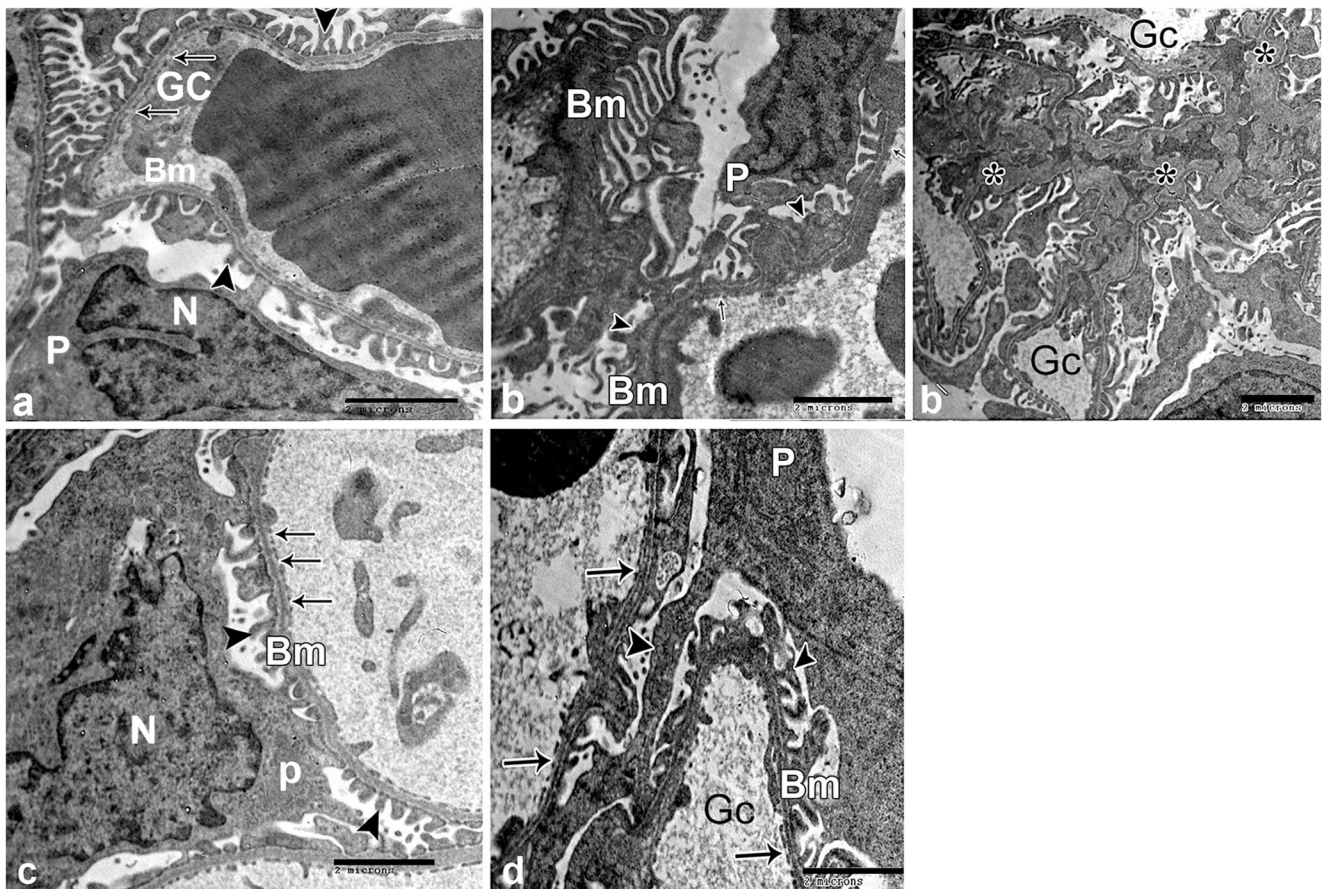


**Fig. 11** Transmission electron micrographs of renal glomeruli. **a** The blood renal barrier of control rat demonstrating glomerular blood capillary (Gc) in which red blood corpuscles reside and lined by fenestrated endothelium (↑). Basement membrane shows regular uniform thickness (Bm). Podocyte (P) with euchromatic nucleus (n) and foot processes (arrow head) are observed. **b** The blood renal barrier of GNT-treated group showing podocytes (P) with distorted foot processes, (arrow head) unapparent filtration slits, irregularly thickened basement membrane (BM) and ill-defined endothelial fenestrations (↑). **b** Glomerular capillaries (Gc) of GNT-treated group showing deposition

of hyaline material in the messangium (\*). **c** The blood renal barrier of UCDA-treated rats showing podocytes (P) with euchromatic nucleus (N) and secondary foot processes (arrow head) with filtration slits in between. Fenestrated endothelium (↑) and regular thickness of basement membrane (Bm) are observed. **d** The blood renal barrier of UCDA-pretreated rats showing a podocyte (P) extending its primary and secondary foot processes (arrow head) in between glomerular capillaries (Gc). Basement membrane (BM) shows uniform thickness. Endothelial fenestrations are well-defined (↑). Scale bars = 2 μm

Our results show that GNT increased the expression of NF- $\kappa$ B (Fig. 4c). NF- $\kappa$ B is the key transcription factor in renal inflammation and regulates the expression of cytokines and adhesion molecules that lead to renal damage (Bae et al. 2014; Sahu et al. 2014a). In the present study, we showed that UDCA decreased the GNT-induced expression of NF- $\kappa$ B (Fig. 4c). Our finding suggests that pretreatment with UDCA significantly alleviates GNT-induced inflammation by modulating the expression of NF- $\kappa$ B. Interestingly, NF- $\kappa$ B is a downstream effector to mitogen-activated protein kinase (MAPK) (Lee et al. 2013; Stambe et al. 2003). More importantly, Ko et al. (2018) demonstrated that UDCA suppressed p38 MAPK activation. Altogether, the anti-inflammatory effect of UDCA could be through inhibition of the p38 MAPK/NF- $\kappa$ B pathway. This role of UDCA needs to be further explored in our model.

An important mechanism that underlies GNT-induced renal damage is inflammation. In this regard, GNT injection releases various inflammatory mediators including chemokines and adhesion molecules (Akcaay et al. 2009; Bledsoe et al. 2006; Tang et al. 1994). Interestingly, the expression of these mediators is TNF- $\alpha$ -dependent (Burne et al. 2001; Ramesh and Reeves 2002). Importantly, elevated TNF- $\alpha$  levels are associated with the activation of NF- $\kappa$ B (Bae et al. 2014; Sahu et al. 2014a). We (Fig. 7b) and others (Bledsoe et al. 2006) showed inflammatory cell infiltration in animals treated with GNT. We also observed increased renal tissue levels of MPO (Fig. 4a) indicative of neutrophil accumulation at the site of tissue injury. The dark side of neutrophil infiltration is that they secrete ROS that destroy the glomerular barrier and renal tubular cells with subsequent deterioration of the kidney function (Linas et al. 1988). Additionally, Bledsoe



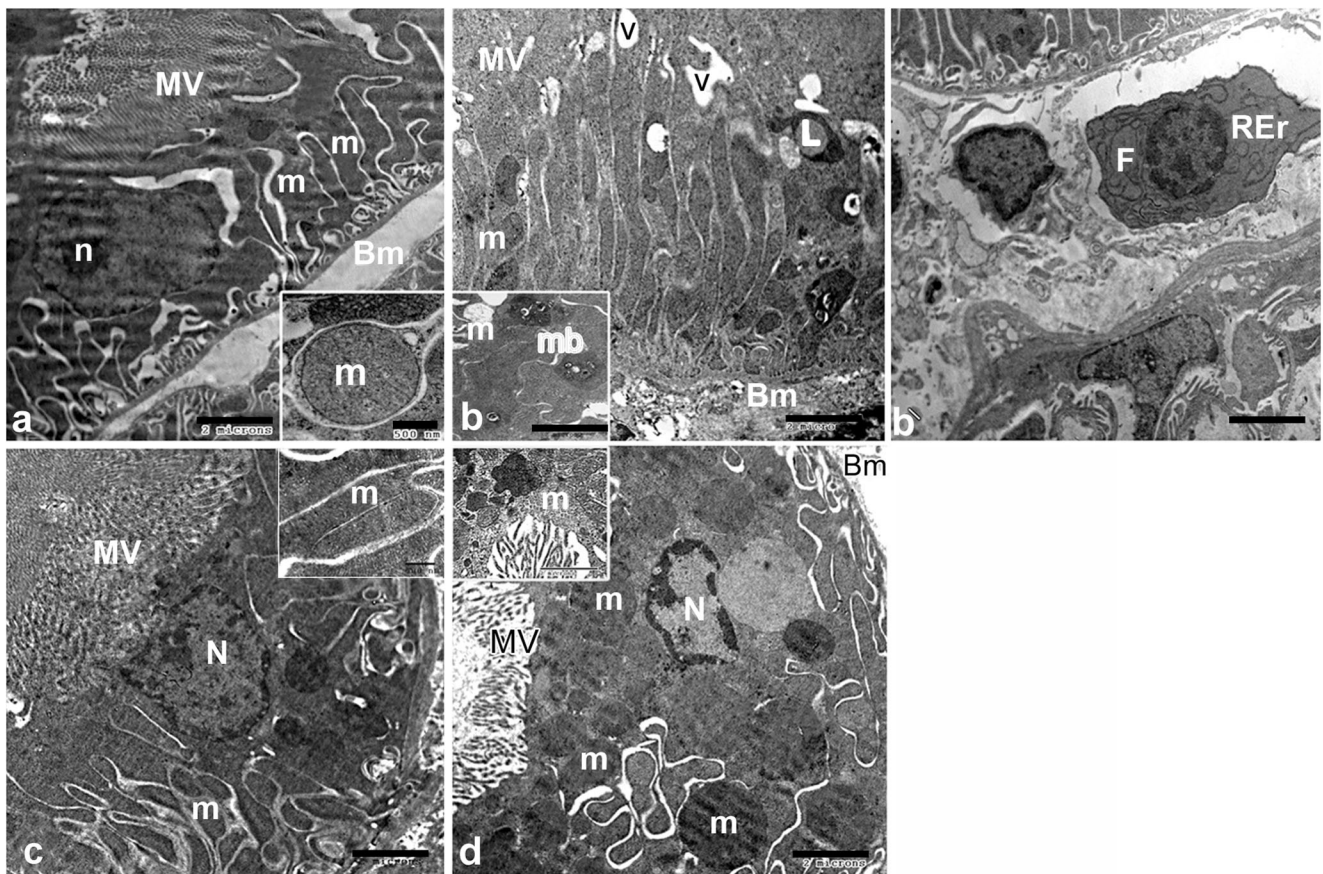


**Fig. 12** Transmission electron micrographs showing proximal convoluted tubule ultrastructure. **a** Proximal convoluted tubule of control rat with well-defined microvilli at the apical border (MV), prominent nucleolus (n) and basal infoldings housing numerous elongated mitochondria (m). Tubular basement membrane is regular and of uniform thickness (Bm). Inset shows normal mitochondrial cristae (m). **b** Proximal convoluted tubule of GNT-treated rat with ill-defined microvilli at the apical border (MV), multiple vacuoles (v), lysosomes (L) and swollen mitochondria (m) thickening of the basement membrane (Bm). Inset shows myeloid bodies (mb) and mitochondria with total cristae

disintegration (m). **b** Renal interstitium of GNT-treated group having a fibroblast (F) with dilated rough endoplasmic reticulum cisternae (REr). **c** Proximal convoluted tubule of UCDA-treated rats with microvilli at the apical border (MV), euchromatic nucleus (N) and mitochondria (m). Inset shows mitochondrial profiles (m) with preserved cristae. **d** Proximal convoluted tubule of UCDA-pretreated rats showing an euchromatic rounded nucleus (N), reappearance of apical microvilli (MV), some swollen mitochondria (m) and normal thickness of the tubular basement membrane (Bm). Inset shows other healthy mitochondria with well-defined cristae (m). Scale bars = 2  $\mu$ m except the inset in **a** and **c** with scale bars = 5 nm

et al. (2006) demonstrated that GNT administration induces monocyte/macrophage migration to the site of tissue damage. This migration could account for the cellular infiltration we observed here. In contrast, pretreatment with UDCA decreased GNT-induced renal tissue infiltration with inflammatory cells (Fig. 7d). In addition, pretreatment with UDCA significantly decreased GNT-induced elevated MPO levels (Fig. 4a). This UDCA effect on inflammatory cell infiltration could be due to suppression of inflammatory cytokines through inactivation of NF- $\kappa$ B. These data further suggest an anti-inflammatory role for UDCA.

Nitric oxide (NO) has physiological and pathological roles in many mammalian cells and tissues (Patel et al. 1999). Previously, it has been shown that basal release of NO is important for renal functions (Kurihara et al. 2002; Radermacher et al. 1992). Nevertheless, overproduction of NO is associated

with oxidative stress (Araujo and Welch 2006). In the present study, we observed increased levels of NOx indicative of increased production of NO (Fig. 3d). This overproduction of NO has been linked to increased expression of iNOS (Buffoli et al. 2005) induced by GNT (Ghaznavi and Kadkhodae 2007). The eNOS however produces a small amount of NO needed for its physiological functions (Raj and Baylis 1995). Here, we demonstrated that GNT reduced eNOS expression (Fig. 5b,e). In contrast, pretreatment with UDCA reversed the effect of GNT on NO production (Fig. 3d) and eNOS expression (Fig. 5d,e). Interestingly, Furuu et al. (1998) demonstrated that expression of eNOS is negatively correlated with the degree of renal damage in experimental animals. Surprisingly, our results show that treating rats with UDCA increased eNOS expression compared to control animals (Fig. 5c,e). This observation is in line with a previously published report by Ko et

al. (2017) who demonstrated that administration of UDCA alone increased NO production by macrophages in vitro in a dose-dependent manner. One speculation about this observation is that UDCA directly increased the expression of eNOS by endothelial cells as well as tubular cells.

Our immunohistochemical analysis reveals that GNT injection significantly increased renal expression of caspase-3 (Fig. 6b,e). This finding was associated with the ultrastructural changes at the tubular level, including loss of microvilli, cytoplasmic vacuolization, abnormal mitochondria and accumulation of lysosomes and myeloid bodies (Fig. 12b). Activation of caspase-3 results in DNA fragmentation (Kumari and Kakkar 2012). Caspase-3 is activated by cleaved caspase-9 (Padanilam 2003), which is activated by the release of cytochrome c (Jiang and Wang 2004). Previously, it has been suggested that GNT induced cytochrome c efflux through opening of mitochondrial permeability transition (MPT) pores in the mitochondrial membrane (Morales et al. 2010). Moreover, Sepand et al. (2016) documented that GNT-induced oxidative stress was accompanied by caspase-3 activation. Furthermore, Li et al. (2018) demonstrated that expression of cleaved caspase-3 was associated with NF- $\kappa$ B activation. In the present study, pretreatment with UDCA significantly reduced GNT-induced caspase-3 expression (Fig. 6d,e). Additionally, UDCA pretreatment decreased GNT-induced tubular changes (Fig. 12d). These observations are in line with the findings of Chen et al. (2011). In addition, several in vivo and in vitro studies have shown that UDCA protects cells against apoptosis by inhibiting caspase-3 activation (Amaral et al. 2007; Cao et al. 2016b; Perez et al. 2006). Moreover, we showed here that pretreatment with UDCA reduced GNT-induced oxidative stress (Fig. 3a–c). Furthermore, we demonstrated that pretreatment with UDCA decreased the GNT-induced NF- $\kappa$ B expression (Fig. 4c). Taken together, reduction of caspase-3 expression with UDCA could be due to reduction of GNT-induced oxidative stress and/or expression of NF- $\kappa$ B.

According to our histological data, treatment of rats with GNT induced significant renal damage. The GNT-induced damage mostly affects the proximal tubules. Here, we observed loss of brush border, vacuolation of tubular cell cytoplasm, desquamated epithelial cells and basement membrane breakdown (Figs. 8 and 9). These observations are in line with previously published reports (Ozbek et al. 2009; Polat et al. 2006; Quiros et al. 2016). GNT is preferentially accumulated in the proximal convoluted tubules (Lopez-Novoa et al. 2011) and localized in the lysosomes (Giurgea-Marion et al. 1986) with subsequent lysosomal rupture and tubular cell damage (El Mouedden et al. 2000). Additionally, cytokines and chemokines released by damaged cells recruit inflammatory cells to the site of injury that aggravate renal damage (Quiros et al. 2011). Moreover, GNT enhances ROS production with subsequent tubular damage through lipid peroxidation (Adil et

al. 2016; Ozbek et al. 2009; Yanagida et al. 2004). Furthermore, accumulating evidences suggest involvement of apoptosis in GNT-induced tubular damage (Juan et al. 2007; Promsan et al. 2016; Sahu et al. 2014b). Interestingly, Volpini et al. (2004) documented that blocking of NF- $\kappa$ B activation attenuates the GNT-induced structural changes. Therefore, controlling GNT-induced oxidative stress, inflammation and apoptosis could alleviate GNT-induced tubular damage. Here, we demonstrated that pretreatment with UDCA decreased GNT-induced morphological changes (Figs. 8 and 9). This could be due to restoring the renal levels of MDA (Fig. 3a), GSH (Fig. 3b), SOD (Fig. 3c), MPO (Fig. 4a) and NF- $\kappa$ B mRNA (Fig. 4c) to the control levels.

Fortunately, UDCA was approved by the FDA in 1997 for the treatment of patients with primary biliary cirrhosis (<https://www.fda.gov> and we used ursodeoxycholic acid as search words). Therefore, clinical use of UDCA for patients with kidney diseases that involve oxidative stress, inflammation and apoptosis can take a rapid and easy path.

In conclusion, we showed that pretreatment with UDCA alleviates the GNT-induced functional and structural changes in rat kidney. UDCA reversed GNT-induced changes in kidney function markers. UDCA also reversed GNT-induced changes in renal levels of MDA, GSH, SOD, MPO, NF- $\kappa$ B and KIM-1 mRNA, eNOS and caspase-3 proteins. Additionally, UDCA decreased the GNT-induced tubular damage. Our results suggest that UDCA may have a therapeutic potential for patients with kidney diseases that are associated with oxidative stress, inflammation and apoptosis. Further animal and human studies are required to support our suggestion.

**Acknowledgements** The authors would like to thank Dr. Adel Maklad from the College of Medicine and Life Sciences, University of Toledo, Toledo, Ohio, USA, for reviewing the language of the manuscript.

## Compliance with ethical standards

**Conflict of interest** The authors declare that they have no conflict of interest.

## References

- Abdel-Raheem IT, Abdel-Ghany AA, Mohamed GA (2009) Protective effect of quercetin against gentamicin-induced nephrotoxicity in rats. *Biol Pharm Bull* 32:61–67
- Adil M, Kandhare AD, Dalvi G, Ghosh P, Venkata S, Raygude KS, Bodhankar SL (2016) Ameliorative effect of berberine against gentamicin-induced nephrotoxicity in rats via attenuation of oxidative stress, inflammation, apoptosis and mitochondrial dysfunction. *Ren Fail* 38:996–1006
- Akao Y, Maruyama W, Shimizu S, Yi H, Nakagawa Y, Shamoto-Nagai M, Youdim MB, Tsujimoto Y, Naoi M (2002) Mitochondrial permeability transition mediates apoptosis induced by N-methyl(R)salsolinol, an endogenous neurotoxin, and is inhibited



- by Bcl-2 and rasagiline, N-propargyl-1(R)-aminoindan. *J Neurochem* 82:913–923
- Akbulut S, Elbe H, Eris C, Dogan Z, Toprak G, Yalcin E, Otan E, Turkoz Y (2015) Effects of antioxidant agents against cyclosporine-induced hepatotoxicity. *J Surg Res* 193:658–666
- Akçay A, Nguyen Q, Edelstein CL (2009) Mediators of inflammation in acute kidney injury. *Mediat Inflamm* 2009:137072
- Amaral JD, Castro RE, Sola S, Steer CJ, Rodrigues CM (2007) p53 is a key molecular target of ursodeoxycholic acid in regulating apoptosis. *J Biol Chem* 282:34250–34259
- Appel GB (1990) Aminoglycoside nephrotoxicity. *Am J Med* 88:16S–20S
- Araujo M, Welch WJ (2006) Oxidative stress and nitric oxide in kidney function. *Curr Opin Nephrol Hypertens* 15:72–77
- Atici S, Cinel I, Cinel L, Doruk N, Eskandari G, Oral U (2005) Liver and kidney toxicity in chronic use of opioids: an experimental long term treatment model. *J Biosci* 30:245–252
- Bae EH, Kim IJ, Joo SY, Kim EY, Choi JS, Kim CS, Ma SK, Lee J, Kim SW (2014) Renoprotective effects of the direct renin inhibitor aliskiren on gentamicin-induced nephrotoxicity in rats. *J Renin-Angiotensin-Aldosterone Syst* 15:348–361
- Balakumar P, Rohilla A, Thangathirupathi A (2010) Gentamicin-induced nephrotoxicity: do we have a promising therapeutic approach to blunt it? *Pharmacol Res* 62:179–186
- Baliga R, Ueda N, Walker PD, Shah SV (1999) Oxidant mechanisms in toxic acute renal failure. *Drug Metab Rev* 31:971–997
- Bartels H, Bohmer M, Heierli C (1972) Serum creatinine determination without protein precipitation. *Clin Chim Acta* 37:193–197
- Baum N, Dichoso CC, Carlton CE (1975) Blood urea nitrogen and serum creatinine. Physiology and interpretations. *Urology* 5:583–588
- Bledsoe G, Crickman S, Mao J, Xia CF, Murakami H, Chao L, Chao J (2006) Kallikrein/kinin protects against gentamicin-induced nephrotoxicity by inhibition of inflammation and apoptosis. *Nephrol Dial Transplant* 21:624–633
- Bozzola JJ (1998) Electron microscopy: principles and techniques for biologists, Second edn. Jones and Bartlett Publishers, Inc., USA
- Buffoli B, Pechanova O, Kojsova S, Andriantsitohaina R, Giugno L, Bianchi R, Rezzani R (2005) Proximal prevents CsA-induced nephrotoxicity by reducing reactive oxygen species, iNOS, and NF- $\kappa$ B expression. *J Histochem Cytochem* 53:1459–1468
- Burne MJ, Elghandour A, Haq M, Saba SR, Norman J, Condon T, Bennett F, Rabb H (2001) IL-1 and TNF independent pathways mediate ICAM-1/VCAM-1 up-regulation in ischemia reperfusion injury. *J Leukoc Biol* 70:192–198
- Buryova H, Chalupsky K, Zbodakova O, Kanchev I, Jirouskova M, Gregor M, Sedlacek R (2013) Liver protective effect of ursodeoxycholic acid includes regulation of ADAM17 activity. *BMC Gastroenterol* 13:155
- Cao A, Wang L, Chen X, Guo H, Chu S, Zhang X, Peng W (2016a) Ursodeoxycholic acid ameliorated diabetic nephropathy by attenuating hyperglycemia-mediated oxidative stress. *Biol Pharm Bull* 39:1300–1308
- Cao AL, Wang L, Chen X, Wang YM, Guo HJ, Chu S, Liu C, Zhang XM, Peng W (2016b) Ursodeoxycholic acid and 4-phenylbutyrate prevent endoplasmic reticulum stress-induced podocyte apoptosis in diabetic nephropathy. *Lab Invest* 96:610–622
- Chen Q, Cui Y, Ding G, Jia Z, Zhang Y, Zhang A, Huang S (2017) PEA3 protects against gentamicin nephrotoxicity: role of mitochondrial dysfunction. *Am J Transl Res* 9:2153–2162
- Chen X, Xu J, Zhang C, Yu T, Wang H, Zhao M, Duan ZH, Zhang Y, Xu JM, Xu DX (2011) The protective effects of ursodeoxycholic acid on isoniazid plus rifampicin induced liver injury in mice. *Eur J Pharmacol* 659:53–60
- Chun HS, Low WC (2012) Ursodeoxycholic acid suppresses mitochondria-dependent programmed cell death induced by sodium nitroprusside in SH-SY5Y cells. *Toxicology* 292:105–112
- Cui S, Verroust PJ, Moestrup SK, Christensen EI (1996) Megalin/gp330 mediates uptake of albumin in renal proximal tubule. *Am J Physiol* 271:F900–F907
- Davies J, Davis BD (1968) Misreading of ribonucleic acid code words induced by aminoglycoside antibiotics. The effect of drug concentration. *J Biol Chem* 243:3312–3316
- de-Barros-e-Silva ML, Varanda WA, Lachat JJ, Alves-da-Silva CG, Coimbra TM (1992) Glomerular permeability to macromolecules in gentamicin-treated rats. *Braz J Med Biol Res* 25:409–417
- Drury RAB, Wallington EA (1980) Carleton's histological technique, 5th edn. Oxford University Press, Oxford, New York, Toronto
- Dumas BT, Watson WA, Biggs HG (1997) Albumin standards and the measurement of serum albumin with bromocresol green. *Clin Chim Acta* 258:21–30
- Edson RS, Terrell CL (1999) The aminoglycosides. *Mayo Clin Proc* 74:519–528
- El Mouedden M, Laurent G, Mingeot-Leclercq MP, Taper HS, Cumps J, Tulkens PM (2000) Apoptosis in renal proximal tubules of rats treated with low doses of aminoglycosides. *Antimicrob Agents Chemother* 44:665–675
- Ellman GL (1959) Tissue sulfhydryl groups. *Arch Biochem Biophys* 82:70–77
- Erdem A, Gundogan NU, Usubutun A, Kilinc K, Erdem SR, Kara A, Bozkurt A (2000) The protective effect of taurine against gentamicin-induced acute tubular necrosis in rats. *Nephrol Dial Transplant* 15:1175–1182
- Fawcett JK, Scott JE (1960) A rapid and precise method for the determination of urea. *J Clin Pathol* 13:156–159
- Furusu A, Miyazaki M, Abe K, Tsukasaki S, Shiohita K, Sasaki O, Miyazaki K, Ozono Y, Koji T, Harada T, Sakai H, Kohno S (1998) Expression of endothelial and inducible nitric oxide synthase in human glomerulonephritis. *Kidney Int* 53:1760–1768
- Ghaznavi R, Kadkhodae M (2007) Comparative effects of selective and non-selective nitric oxide synthase inhibition in gentamicin-induced rat nephrotoxicity. *Arch Toxicol* 81:453–457
- Giurgea-Marion L, Toubeau G, Laurent G, Heuson-Stiennon JA, Tulkens PM (1986) Impairment of lysosome-pinosome vesicle fusion in rat kidney proximal tubules after treatment with gentamicin at low doses. *Toxicol Appl Pharmacol* 86:271–285
- Gorritz JL, Martinez-Castelao A (2012) Proteinuria: detection and role in native renal disease progression. *Transplant Rev (Orlando)* 26:3–13
- Han WK, Bailly V, Abichandani R, Thadhani R, Bonventre JV (2002) Kidney injury molecule-1 (KIM-1): a novel biomarker for human renal proximal tubule injury. *Kidney Int* 62:237–244
- Hosaka EM, Santos OF, Seguro AC, Vattimo MF (2004) Effect of cyclooxygenase inhibitors on gentamicin-induced nephrotoxicity in rats. *Braz J Med Biol Res* 37:979–985
- Ikari A, Nagatani Y, Tsukimoto M, Harada H, Miwa M, Takagi K (2005) Sodium-dependent glucose transporter reduces peroxynitrite and cell injury caused by cisplatin in renal tubular epithelial cells. *Biochim Biophys Acta* 1717:109–117
- Ikegami T, Matsuzaki Y (2008) Ursodeoxycholic acid: mechanism of action and novel clinical applications. *Hepatol Res* 38:123–131
- Jia P, Teng J, Zou J, Fang Y, Jiang S, Yu X, Krieger AJ, Liang M, Ding X (2013) Intermittent exposure to xenon protects against gentamicin-induced nephrotoxicity. *PLoS One* 8:e64329
- Jiang X, Wang X (2004) Cytochrome C-mediated apoptosis. *Annu Rev Biochem* 73:87–106
- Jose SP, A S, K IM, R M, Santhosh S, S S, K GB, P C (2017) Nephroprotective effect of a novel formulation of unopened coconut inflorescence sap powder on gentamicin induced renal damage by modulating oxidative stress and inflammatory markers. *Biomed Pharmacother* 85:128–135
- Juan SH, Chen CH, Hsu YH, Hou CC, Chen TH, Lin H, Chu YL, Sue YM (2007) Tetramethylpyrazine protects rat renal tubular cell apoptosis induced by gentamicin. *Nephrol Dial Transplant* 22:732–739

- Kalayarasan S, Prabhu PN, Sriram N, Manikandan R, Arumugam M, Sudhandiran G (2009) Diallyl sulfide enhances antioxidants and inhibits inflammation through the activation of Nrf2 against gentamicin-induced nephrotoxicity in Wistar rats. *Eur J Pharmacol* 606:162–171
- Ko WK, Kim SJ, Jo MJ, Choi H, Lee D, Kwon IK, Lee SH, Han IB, Sohn S (2018) Ursodeoxycholic acid inhibits inflammatory responses and promotes functional recovery after spinal cord injury in rats. *Mol Neurobiol*
- Ko WK, Lee SH, Kim SJ, Jo MJ, Kumar H, Han IB, Sohn S (2017) Anti-inflammatory effects of ursodeoxycholic acid by lipopolysaccharide-stimulated inflammatory responses in RAW 264.7 macrophages. *PLoS One* 12:e0180673
- Kumari A, Kakkur P (2012) Upeol prevents acetaminophen-induced in vivo hepatotoxicity by altering the Bax/Bcl-2 and oxidative stress-mediated mitochondrial signaling cascade. *Life Sci* 90:561–570
- Kurihara N, Yanagisawa H, Sato M, Tien CK, Wada O (2002) Increased renal vascular resistance in zinc-deficient rats: role of nitric oxide and superoxide. *Clin Exp Pharmacol Physiol* 29:1096–1104
- Lapenna D, Ciofani G, Festi D, Neri M, Pierdomenico SD, Giamberardino MA, Cuccurullo F (2002) Antioxidant properties of ursodeoxycholic acid. *Biochem Pharmacol* 64:1661–1667
- Laurent G, Kishore BK, Tulkens PM (1990) Aminoglycoside-induced renal phospholipidosis and nephrotoxicity. *Biochem Pharmacol* 40:2383–2392
- Lee IC, Kim SH, Lee SM, Baek HS, Moon C, Kim SH, Park SC, Kim HC, Kim JC (2012) Melatonin attenuates gentamicin-induced nephrotoxicity and oxidative stress in rats. *Arch Toxicol* 86:1527–1536
- Lee KE, Kim EY, Kim CS, Choi JS, Bae EH, Ma SK, Kim KK, Lee JU, Kim SW (2013) Macrophage-stimulating protein attenuates gentamicin-induced inflammation and apoptosis in human renal proximal tubular epithelial cells. *Biochem Biophys Res Commun* 434:527–533
- Li J, Li L, Wang S, Zhang C, Zheng L, Jia Y, Xu M, Zhu T, Zhang Y, Rong R (2018) Resveratrol alleviates inflammatory responses and oxidative stress in rat kidney ischemia-reperfusion injury and H<sub>2</sub>O<sub>2</sub>-induced NRK-52E cells via the Nrf2/TLR4/NF-kappaB pathway. *Cell Physiol Biochem* 45:1677–1689
- Linan SL, Shanley PF, Whittenburg D, Berger E, Repine JE (1988) Neutrophils accentuate ischemia-reperfusion injury in isolated perfused rat kidneys. *Am J Phys* 255:F728–F735
- Lopez-Novoa JM, Quiros Y, Vicente L, Morales AI, Lopez-Hernandez FJ (2011) New insights into the mechanism of aminoglycoside nephrotoxicity: an integrative point of view. *Kidney Int* 79:33–45
- Luft FC, Yum MN, Walker PD, Kleit SA (1977) Gentamicin gradient patterns and morphological changes in human kidneys. *Nephron* 18:167–174
- Luo QH, Chen ML, Chen ZL, Huang C, Cheng AC, Fang J, Tang L, Geng Y (2016) Evaluation of KIM-1 and NGAL as early indicators for assessment of gentamycin-induced nephrotoxicity in vivo and in vitro. *Kidney Blood Press Res* 41:911–918
- Maldonado PD, Barrera D, Medina-Campos ON, Hernandez-Pando R, Ibarra-Rubio ME, Pedraza-Chaverri J (2003) Aged garlic extract attenuates gentamicin induced renal damage and oxidative stress in rats. *Life Sci* 73:2543–2556
- Manktelow A, Meyer AA (1986) Lack of correlation between decreased chemotaxis and susceptibility to infection in burned rats. *J Trauma* 26:143–148
- Marklund SL (1985) Superoxide dismutase isoenzymes in tissues and plasma from New Zealand black mice, nude mice and normal BALB/c mice. *Mutat Res* 148:129–134
- Mihara M, Uchiyama M (1978) Determination of malonaldehyde precursor in tissues by thiobarbituric acid test. *Anal Biochem* 86:271–278
- Mitsuyoshi H, Nakashima T, Sumida Y, Yoh T, Nakajima Y, Ishikawa H, Inaba K, Sakamoto Y, Okanoue T, Kashima K (1999) Ursodeoxycholic acid protects hepatocytes against oxidative injury via induction of antioxidants. *Biochem Biophys Res Commun* 263:537–542
- Montgomery HAC, Dymock JF (1961) The determination of nitrite in water: colorimetric method of nitric oxide assay. *Analyst* 86:414
- Morales AI, Detaille D, Prieto M, Puente A, Briones E, Arevalo M, Lerverve X, Lopez-Novoa JM, El-Mir MY (2010) Metformin prevents experimental gentamicin-induced nephropathy by a mitochondria-dependent pathway. *Kidney Int* 77:861–869
- Morsy MA, Ibrahim SA, Amin EF, Kamel MY, Rifaai RA, Hassan MK (2014) Sildenafil ameliorates gentamicin-induced nephrotoxicity in rats: role of iNOS and eNOS. *J Toxicol* 2014:489382
- Nagai J, Saito M, Adachi Y, Yumoto R, Takano M (2006) Inhibition of gentamicin binding to rat renal brush-border membrane by megalin ligands and basic peptides. *J Control Release* 112:43–50
- Nagai J, Takano M (2004) Molecular aspects of renal handling of aminoglycosides and strategies for preventing the nephrotoxicity. *Drug Metab Pharmacokinet* 19:159–170
- Okada K, Shoda J, Taguchi K, Maher JM, Ishizaki K, Inoue Y, Ohtsuki M, Goto N, Takeda K, Utsunomiya H, Oda K, Warabi E, Ishii T, Osaka K, Hyodo I, Yamamoto M (2008) Ursodeoxycholic acid stimulates Nrf2-mediated hepatocellular transport, detoxification, and antioxidative stress systems in mice. *Am J Physiol Gastrointest Liver Physiol* 295:G735–G747
- Osorio H, Coronel I, Arellano A, Franco M, Escalante B, Bautista R (2012) Ursodeoxycholic acid decreases sodium-glucose cotransporter (SGLT2) expression and oxidative stress in the kidney of diabetic rats. *Diabetes Res Clin Pract* 97:276–282
- Otunctemur A, Ozbek E, Cekmen M, Cakir SS, Dursun M, Polat EC, Somay A, Ozbay N (2013) Protective effect of montelukast which is cysteinyl-leukotriene receptor antagonist on gentamicin-induced nephrotoxicity and oxidative damage in rat kidney. *Ren Fail* 35:403–410
- Ou HC, Lee WJ, Lee SD, Huang CY, Chiu TH, Tsai KL, Hsu WC, Sheu WH (2010) Ellagic acid protects endothelial cells from oxidized low-density lipoprotein-induced apoptosis by modulating the PI3K/Akt/eNOS pathway. *Toxicol Appl Pharmacol* 248:134–143
- Ozbek E, Cekmen M, Ilbey YO, Simsek A, Polat EC, Somay A (2009) Atorvastatin prevents gentamicin-induced renal damage in rats through the inhibition of p38-MAPK and NF-kappaB pathways. *Ren Fail* 31:382–392
- Padanilam BJ (2003) Cell death induced by acute renal injury: a perspective on the contributions of apoptosis and necrosis. *Am J Physiol Renal Physiol* 284:F608–F627
- Patel RP, McAndrew J, Sellak H, White CR, Jo H, Freeman BA, Darley-Usmar VM (1999) Biological aspects of reactive nitrogen species. *Biochim Biophys Acta* 1411:385–400
- Pattyn VM, Verpooten GA, Giuliano RA, Zheng F, De Broe ME (1988) Effect of hyperfiltration, proteinuria and diabetes mellitus on the uptake kinetics of gentamicin in the kidney cortex of rats. *J Pharmacol Exp Ther* 244:694–698
- Perez MJ, Macias RI, Marin JJ (2006) Maternal cholestasis induces placental oxidative stress and apoptosis. Protective effect of ursodeoxycholic acid. *Placenta* 27:34–41
- Polat A, Parlakpınar H, Tasdemir S, Colak C, Vardi N, Ucar M, Emre MH, Acet A (2006) Protective role of aminoguanidine on gentamicin-induced acute renal failure in rats. *Acta Histochem* 108:365–371
- Poupon R (2012) Ursodeoxycholic acid and bile-acid mimetics as therapeutic agents for cholestatic liver diseases: an overview of their mechanisms of action. *Clin Res Hepatol Gastroenterol* 36(Suppl 1):S3–S12
- Priuska EM, Schacht J (1995) Formation of free radicals by gentamicin and iron and evidence for an iron/gentamicin complex. *Biochem Pharmacol* 50:1749–1752
- Promsan S, Jaikumkao K, Pongchaidecha A, Chattipakorn N, Chatsudthipong V, Arjinajarn P, Pompimon W, Lungkaphin A



- (2016) Pinocembrin attenuates gentamicin-induced nephrotoxicity in rats. *Can J Physiol Pharmacol* 94:808–818
- Quiros Y, Blanco-Gozalo V, Sanchez-Gallego JI, Lopez-Hernandez FJ, Ruiz J, Perez de Obanos MP, Lopez-Novoa JM (2016) Cardiotrophin-1 therapy prevents gentamicin-induced nephrotoxicity in rats. *Pharmacol Res* 107:137–146
- Quiros Y, Vicente-Vicente L, Morales AI, Lopez-Novoa JM, Lopez-Hernandez FJ (2011) An integrative overview on the mechanisms underlying the renal tubular cytotoxicity of gentamicin. *Toxicol Sci* 119:245–256
- Rademacher J, Klanke B, Schurek HJ, Stolte HF, Frolich JC (1992) Importance of NO/EDRF for glomerular and tubular function: studies in the isolated perfused rat kidney. *Kidney Int* 41:1549–1559
- Raij L, Baylis C (1995) Glomerular actions of nitric oxide. *Kidney Int* 48:20–32
- Ramesh G, Reeves WB (2002) TNF-alpha mediates chemokine and cytokine expression and renal injury in cisplatin nephrotoxicity. *J Clin Invest* 110:835–842
- Rodrigues CM, Fan G, Wong PY, Kren BT, Steer CJ (1998) Ursodeoxycholic acid may inhibit deoxycholic acid-induced apoptosis by modulating mitochondrial transmembrane potential and reactive oxygen species production. *Mol Med* 4:165–178
- Sahu BD, Kalvala AK, Koneru M, Mahesh KJ, Kuncha M, Rachamalla SS, Sistla R (2014a) Ameliorative effect of fisetin on cisplatin-induced nephrotoxicity in rats via modulation of NF-kappaB activation and antioxidant defence. *PLoS One* 9:e105070
- Sahu BD, Tatireddy S, Koneru M, Borkar RM, Kumar JM, Kuncha M, Srinivas R, Shyam SR, Sistla R (2014b) Naringin ameliorates gentamicin-induced nephrotoxicity and associated mitochondrial dysfunction, apoptosis and inflammation in rats: possible mechanism of nephroprotection. *Toxicol Appl Pharmacol* 277:8–20
- Sandoval RM, Molitoris BA (2004) Gentamicin traffics retrograde through the secretory pathway and is released in the cytosol via the endoplasmic reticulum. *Am J Physiol Renal Physiol* 286:F617–F624
- Sardana A, Kalra S, Khanna D, Balakumar P (2015) Nephroprotective effect of catechin on gentamicin-induced experimental nephrotoxicity. *Clin Exp Nephrol* 19:178–184
- Schrier RW, Wang W, Poole B, Mitra A (2004) Acute renal failure: definitions, diagnosis, pathogenesis, and therapy. *J Clin Invest* 114:5–14
- Selby NM, Shaw S, Woodier N, Fluck RJ, Kolhe NV (2009) Gentamicin-associated acute kidney injury. *QJM* 102:873–880
- Sepand MR, Ghahremani MH, Razavi-Azarkhiavi K, Aghsami M, Rajabi J, Keshavarz-Bahaghighat H, Soodi M (2016) Ellagic acid confers protection against gentamicin-induced oxidative damage, mitochondrial dysfunction and apoptosis-related nephrotoxicity. *J Pharm Pharmacol* 68:1222–1232
- Shi KQ, Fan YC, Liu WY, Li LF, Chen YP, Zheng MH (2012) Traditional Chinese medicines benefit to nonalcoholic fatty liver disease: a systematic review and meta-analysis. *Mol Biol Rep* 39:9715–9722
- Shin HS, Yu M, Kim M, Choi HS, Kang DH (2014) Renoprotective effect of red ginseng in gentamicin-induced acute kidney injury. *Lab Invest* 94:1147–1160
- Stambe C, Atkins RC, Tesch GH, Kapoun AM, Hill PA, Schreiner GF, Nikolic-Paterson DJ (2003) Blockade of p38alpha MAPK ameliorates acute inflammatory renal injury in rat anti-GBM glomerulonephritis. *J Am Soc Nephrol* 14:338–351
- Sun J, Hulthenby K, Axelsson J, Nordstrom J, He B, Wernerson A, Lindstrom K (2017) Proximal tubular expression patterns of megalin and cubilin in proteinuric nephropathies. *Kidney Int Rep* 2:721–732
- Tang WW, Feng L, Mathison JC, Wilson CB (1994) Cytokine expression, upregulation of intercellular adhesion molecule-1, and leukocyte infiltration in experimental tubulointerstitial nephritis. *Lab Invest* 70:631–638
- Vaidya VS, Ramirez V, Ichimura T, Bobadilla NA, Bonventre JV (2006) Urinary kidney injury molecule-1: a sensitive quantitative biomarker for early detection of kidney tubular injury. *Am J Physiol Renal Physiol* 290:F517–F529
- Volpini RA, Costa RS, da Silva CG, Coimbra TM (2004) Inhibition of nuclear factor-kappaB activation attenuates tubulointerstitial nephritis induced by gentamicin. *Nephron Physiol* 98:97–106
- Ward JBJ, Lajczak NK, Kelly OB, O'Dwyer AM, Giddam AK, Ni GJ, Franco P, Tambuwala MM, Jefferies CA, Keely S, Roda A, Keely SJ (2017) Ursodeoxycholic acid and lithocholic acid exert anti-inflammatory actions in the colon. *Am J Physiol Gastrointest Liver Physiol* 312:G550–G558
- Watanabe A, Nagai J, Adachi Y, Katsube T, Kitahara Y, Murakami T, Takano M (2004) Targeted prevention of renal accumulation and toxicity of gentamicin by aminoglycoside binding receptor antagonists. *J Control Release* 95:423–433
- Whiting PH, Brown PA (1996) The relationship between enzymuria and kidney enzyme activities in experimental gentamicin nephrotoxicity. *Ren Fail* 18:899–909
- Yanagida C, Ito K, Komiya I, Horie T (2004) Protective effect of fosfomycin on gentamicin-induced lipid peroxidation of rat renal tissue. *Chem Biol Interact* 148:139–147